Atmos. Chem. Phys. Discuss., doi:10.5194/acp-2016-1069, 2016
Manuscript under review for journal Atmos. Chem. Phys.
Published: 15 December 2016

Atmospheric Chemistry and Physics Discussions

Modeling the Physical Multi-Phase Interactions of HNO_3 Between Snow and Air on the Antarctic Plateau (Dome C) and coast (Halley)

Hoi Ga Chan[1,2], Markus M. Frey[1], and Martin D. King[2]

[1]British Antarctic Survey, Natural Environment Research Council, Cambridge, CB3 0ET,UK
[2]Department of Earth Sciences, Royal Holloway University of London, Egham, Surrey, TW20 0EX, UK

Correspondence to: Hoi Ga Chan
(hohan47@bas.ac.uk)

Abstract. Nitrogen oxides (NO_x = NO + NO_2) emissions from nitrate (NO_3^-) photolysis in snow affect the oxidising capacity of the lower troposphere especially in remote regions of the high latitudes with low pollution levels. The porous structure of snowpack allows the exchange of gases with the atmosphere driven by physicochemical processes, and hence, snow can act as both source and sink of atmospheric chemical trace gases. Current models are limited by poor process understanding and often require tuning parameters, for example the recently developed air-snow exchange model by Bock et al. (2016) requires an unrealistically large growth rate of snow grains to explain the NO_3^- peak in surface snow at Dome C in the summer. Here, two multi-phase physical models were developed from first principles constrained by observed atmospheric nitrate, HNO_3, to describe the air-snow interaction of nitrate. Similar to most of the previous approaches, the first model assumes that below a threshold temperature, T_o, the air-snow grain interface is pure ice and above T_o, a disordered interface (DI) emerges assumed to be covering the entire grain surface. The second model assumes that Air-Ice interactions dominate over the entire temperature range below melting and that only above the eutectic temperature, liquid is present in the form of micropockets in grooves. The models are validated with available year-round observations of nitrate in snow and air at a cold site on the Antarctica Plateau (Dome C, $75°06'S, 123°33'E$, 3233 m a.s.l.) and at a relatively warm site on the Antarctica coast (Halley, $75°35'S, 26°39'E$, 35 m a.s.l). The first model agrees reasonably well with observations at Dome C ($C_v(RMSE)$ = 1.34), but performs poorly at Halley ($C_v(RMSE)$ = 89.28) while the second model reproduces with good agreement observations at both sites without any tuning ($C_v(RMSE)$ = 0.84 at both sites). It is therefore suggested that air-snow interactions of nitrate in the winter are determined by non-equilibrium surface adsorption and co-condensation on ice coupled with solid-state diffusion inside the grain, similar to Bock et al. (2016). In summer,

Atmos. Chem. Phys. Discuss., doi:10.5194/acp-2016-1069, 2016
Manuscript under review for journal Atmos. Chem. Phys.
Published: 15 December 2016

Atmospheric Chemistry and Physics Discussions

however, the air-snow exchange of nitrate is mainly driven by solvation into liquid micropockets following Henry's law with contributions to total NO_3^- concentrations of 75% and 80% at Dome C and Halley respectively. It is also found that liquid volume of the snow grain and air-micropocket partitioning of HNO_3 are sensitive to total solute concentration and pH. In conclusion, the second model can be used to predict nitrate concentration in surface snow over the entire range of environmental conditions typical for Antarctica and forms a basis for parameterisations in regional or global atmospheric chemistry models.

1 Introduction

Emissions of nitrogen oxides, NO_x = NO + NO_2, from snow to the overlying air as a result of photolysis of the nitrate anion, NO_3^-, within snow have been observed in polar (Jones et al., 2001; Beine et al., 2002) and midlatitudes regions (Honrath et al., 2000). They were found to have significant impact on the oxidising capacity of the atmospheric boundary layer, especially in remote areas; such as the polar regions, where anthropogenic pollution is rare (Grannas et al., 2007). The cycling of NO and NO_2 in the troposphere alters the concentration of tropospheric ozone, O_3, partitioning of hydroxy radicals, HO_x, and organic peroxy radicals, RO_x. Tropospheric ozone is a pollutant and a greenhouse gas, and changes in the concentration can alter the regional energy balance and therefore climate (Fowler et al., 2008). Conversely, HO_x radicals are responsible for removal of many atmospheric pollutants (Gligorovski et al., 2015), such as the greenhouse gas methane, and RO_x radicals play an important role in the oxidation of volatile organic compounds (VOCs). There is a great need to understand more about the interaction of reactive nitrogen (NO_y = NO_x + HNO_3 + HONO + N_2O_5 + HO_2NO_2 + NO_3 + PAN + Organic Nitrates) between the atmosphere and snowpack, not only to predict the regional and global chemical transport and climate, but also crucial for interpreting the ice core record of NO_3^-. Both chemical and physical (post-)depositional processes have a strong influence on concentration preserved in snow and ice (Röthlisberger et al., 2000), and therefore need to be understood to enable reconstruction of past atmospheric nitrogen from ice core data.

The physical exchange of nitric acid, HNO_3, between the atmosphere or snow interstitial air (SIA) and snow grain is complex. Gaseous HNO_3 can be taken up by different reservoirs in snow, for example it can be diffused into the ice crystal and formed solid solution or be adsorbed on the ice surface or be co-condensed to the growing ice or be dissolved to the liquid solution located in grain boundaries, grooves at triple junctions or quadruple points. Therefore, the air and snow grain form a complex multiphase interface (Bartels-Rausch et al., 2014). Isotopic studies have shown photolysis of NO_3^- is the dominating loss process of NO_3^- in snow (Frey et al., 2009; Erbland et al., 2013). However, the physical uptake processes of NO_3^- are overwhelming the photochemical loss at the skin layer snow (the top few mm of the snowpack). The typical nitrate photolysis rate, $J_{NO_3^-}$, values

Atmos. Chem. Phys. Discuss., doi:10.5194/acp-2016-1069, 2016
Manuscript under review for journal Atmos. Chem. Phys.
Published: 15 December 2016

Atmospheric Chemistry and Physics Discussions

measured in Antarctica in the summer are on the order of 10^{-7} s^{-1}, for example, France et al. (2011) shows the surface snow $J_{NO_3^-} \approx 1 \times 10^{-7}$ s^{-1} in Dome C at a solar zenith angle of 52°, the maximum solar elevation at Dome C. Therefore, in Antarctica the characteristic time for photochemical lost is around 10^7 s. With the general temperature range found in Antarctica, 0° – -60°C, the characteristic time of physical processes such as surface adsorption and solid-state diffusion for HNO_3 are on the order of 10^2-10^3 s and 10^4-10^6 s respectively, much shorter than the characteristic time for the photochemical process. Therefore, photochemical reactions of NO_3^- are neglected in this study.

A quantitative mechanistic understanding of the role of the physical processes is still poor. Models have been developed to predict the coupling between the snowpack and the overlying atmosphere. Some of the 1D air-snow and chemical models assumed an 'Air-Liquid/Disordered Interface' between snow grain and its surrounding air (e.g. Boxe and Saiz-Lopez, 2008; Thomas et al., 2011; Toyota et al., 2014; Murray et al., 2015). The disordered interface, DI, is a thin layer on the surface of the snow grain and, in general, is assumed to have the following characteristics; 1) DI reaction and partition rate constants are similar as those in the aqueous phase, e.g. using Henry's Law coefficient to describe the partitioning between the 2 phases; 2) DI thickness ranges from <1 to a few hundreds nm (Bartels-Rausch et al., 2014) but is often set to an arbitrary value in models, e.g. both Thomas et al., 2011 and Murray et al., 2015 assumed the DI is 10 nm thick; 3) The DI is where all (Toyota et al., 2014) or a fraction (Thomas et al., 2011; Murray et al., 2015) of solutes are located.

Instead of an 'Air-DI' interface, other models assuming the interface between snow grain and surrounding air to be 'Air-Ice' (e.g. Hutterli et al., 2003; Bock et al., 2016). The distribution of hydrogen peroxide, H_2O_2, and formaldehyde, HCHO, been estimated using a physical air-snow-firn transfer model which included a temperature driven 'Air-Ice' uptake and release (Hutterli et al., 2003; McConnell et al., 1998). The air-ice exchange of H_2O_2 is defined by solid-state diffusion whereas the exchange of HCHO is described by linear adsorption isotherm. The concentration of NO_3^- in the skin layer of the snowpack at Dome C, East Antartica Plateau been estimated using a physical exchange model (Bock et al., 2016). They proposed, at Dome C, the skin layer snow nitrate concentration is determined by thermodynamic equilibrium ice solubility on the grain surface (based on a parameterisation by Thibert et al., 1998) followed by solid-state diffusion during winter. In the summer, the large NO_3^- concentrations in skin layer snow are mainly contributed by co-condensation of H_2O and HNO_3, a kinetic process, rather than equilibrium solubility coupled with solid-state diffusion. Bock et al. (2016) suggest there is no lost of NO_3^- due to co-sublimilation (volatilisation) at all time during the summer, which Röthlisberger et al. (2000) suggested to be one of the important physical processes. A common aspect among all these models mentioned above with an 'Air-DI' or 'Air-Ice' interface, is they require tuning parameters, for example fraction of solute in the DI (Thomas et al., 2011), thickness of the DI (Toyota et al., 2014), ion partitioning coefficients (Hutterli and Röthlisberger, 1999), or co-condensation parameter (Bock et al., 2016), to match the observations and hence limit their predictive capacity.

Atmos. Chem. Phys. Discuss., doi:10.5194/acp-2016-1069, 2016
Manuscript under review for journal Atmos. Chem. Phys.
Published: 15 December 2016

Atmospheric Chemistry and Physics Discussions

The aim of this paper is to develop a physical exchange model from first principles to describe the exchange processes of nitrate between the atmosphere and the skin layer snow without requiring any tuning parameters. Two temperature dependent multi-phase models are developed to evaluate two different concepts to describe the interaction between air and snow nitrate. Model 1 is based on the hypothesis of the existence of a DI layer cover the entire snow grain above a threshold temperature, T_o (Sect. 3.1). Below T_o, the interface between snow grain and air is assumed to be 'Air-Ice', which the NO_3^- concentration is determined by non-equilibrium surface adsorption, in contrast to Bock et al. (2016) equilibrium approach, and co-condensation coupled to solid-state diffusion into the grain. Above T_o, the interface is assumed to be 'Air-DI' of which the NO_3^- concentration is defined by non-equilibrium solvation in DI followed by solid-state diffusion. Model 2 is based on the hypothesis of the co-existence of liquid and ice above the eutectic temperature, T_e, and the liquid is in the form of micropockets located in grooves at grain boundaries or triple junctions (Domine et al., 2013). Therefore, at all temperature below melting the major interface between air and snow grain is assumed to be 'Air-Ice', of which the NO_3^- concentration is described by the same 'Air-Ice' processes mentioned above. In the presence of liquid, i.e. above T_e, the partitioning of HNO_3 to the micropocket is described by equilibrium Henry's Law (Sect. 3.2). The models are validated with data collected at two sites in Antarctica that have very different atmospheric composition, temperature range and humidity; The East Antarctic Plateau at Dome C and secondly coastal Antarctica at Halley, where long term atmospheric and meteorological observations are monitored at the Clean Air Sector Laboratory (CASLab) (Jones et al., 2008).

2 Current Understanding of Air-Snow Physical Processes

2.1 Air-Ice Interface: Surface Adsorption

Adsorption occurs in the ice stability region of the phase diagram. The probability of a gas molecule being adsorbed on a clean surface can be described by the surface accommodation coefficient, α (Crowley et al., 2010). The adsorbed molecule can then be desorbed thermally if the bond to the surface site is weak or it can be diffused into the bulk and form a solid solution. The adsorption of HNO_3 can be explained by single-site Langmuir adsorption even at low HNO_3 partial pressures (Ullerstam et al., 2005b) and the mechanism is as follow:

$$HNO_{3,(g)} + S \underset{k_{des}}{\overset{k_{ads}}{\rightleftharpoons}} HNO_{3,(ads)} \tag{R1}$$

where (g) and (ads) are the gas-phase and surface adsorbed nitrate. [S] is the surface site concentration i.e. number of site available per unit volume of air (Cox et al., 2005) and is defined as follows:

$$[S] = (1-\theta)\, N_{max}\, \frac{A_{ice}}{V_{air}} \tag{1}$$

Atmos. Chem. Phys. Discuss., doi:10.5194/acp-2016-1069, 2016
Manuscript under review for journal Atmos. Chem. Phys.
Published: 15 December 2016

Atmospheric Chemistry and Physics Discussions

Here, θ is the fraction of maximum surface sites being occupied, N_{max} is the maximum number of surface sites with a unit of $\mathrm{molecules\,m_{ice}^{-2}}$, $\mathrm{A_{ice}}$ is the surface area of ice per unit volume of snowpack with a unit of $\mathrm{m_{ice}^2\,m_{snowpack}^{-3}}$, and $\mathrm{V_{air}}$ is the volume of air per unit volume of snowpack with a unit of $\mathrm{m_{air}^3\,m_{snowpack}^{-3}}$. All concentration units are in $\mathrm{molecule\,m^{-3}}$. The adsorption coefficient, k_{ads} ,and desorption coefficient, k_{des}, in R1 can be expressed as

$$k_{\mathrm{ads}} = \frac{\alpha \overline{v}}{4} \frac{1}{N_{max}} \tag{2}$$

$$k_{\mathrm{des}} = \frac{k_{\mathrm{ads}}}{K_{\mathrm{eq}}} \tag{3}$$

Note that k_{ads} has an unit of $\mathrm{m^3\,molecule^{-1}\,s^{-1}}$ while the unit of k_{des} is $\mathrm{s^{-1}}$. Here $\overline{v}$ is the average gas phase molecular speed and K_{eq} is the equilibrium constant for Langmuir adsorption of $\mathrm{HNO_3}$ onto ice with a unit of $\mathrm{m^3\,molecule^{-1}}$. K_{eq} is inversely correlated with temperature that the scavenging efficiency of gas-phase $\mathrm{HNO_3}$ via adsorption increases as temperature decreases. The parameterisations used within this study for α, N_{max}, $\overline{v}$, and K_{eq} are listed in App. A.

2.2 Solid-State diffusion

The nitric acid has a sufficient solubility and diffusivity in ice ($k_{\mathrm{diff}} \approx 7 \times 10^{-15}\ \mathrm{m^2\,s^{-1}}$ at 253 K, Thibert et al., 1998) that a solid solution can be formed. Cox et al. (2005) shows solid-state diffusion of nitrate molecules can occur concurrently with surface adsorption, such that

$$\mathrm{HNO_{3,(ads)}} \overset{k_{\mathrm{diff}}}{\rightleftarrows} \mathrm{HNO_{3,(ice)}} \tag{R2}$$

where k_{diff} is the solid diffusion coefficient (App. A) and (ice) is the nitrate solid state incorporated into the ice matrix. Bartels-Rausch et al. (2014) also concluded that solid-state diffusion in natural snow can be an important process for understanding the partitioning of highly soluble trace gases, such as $\mathrm{HNO_3}$, between atmosphere an snow and when interpreting the composition of environmental ice.

2.3 Coexistence of Liquid Solution with Ice

Liquid aqueous solution coexists with ice in the presence of impurities, such as sea salt and acids, down to the eutectic temperature of ice and the respective impurity. Cho et al. (2002) parameterise the liquid water fraction, $\phi_{\mathrm{H_2O}}$, as function of total ionic concentration and temperature as follows:

$$\phi_{\mathrm{H_2O}}(T) = \frac{\overline{m}_{\mathrm{H_2O}} R T_f}{1000 \Delta H_f^0} \left(\frac{T}{T - T_f} \right) \Phi_{\mathrm{bulk}}^{\mathrm{aq}} \left[\mathrm{Ion_{tot\,(bulk)}} \right] \tag{4}$$

where $\phi_{\mathrm{H_2O}}$ has an unit of $\mathrm{m_{liquid}^3\,m_{ice}^{-3}}$, $\overline{m}_{\mathrm{H_2O}}$ is the molecular weight of water, R is the ideal gas constant, T_f is the freezing temperature of pure water in K, ΔH_f^0 is the enthalpy of fusion in $\mathrm{J\,mol^{-1}}$, $\Phi_{\mathrm{bulk}}^{\mathrm{aq}}$ is the fraction of the total solute in the aqueous phase and $[\mathrm{Ion_{tot,\,bulk}}]$ is the total ionic concentration in the unfrozen bulk. There are different hypothesises on the locations of the

Atmos. Chem. Phys. Discuss., doi:10.5194/acp-2016-1069, 2016
Manuscript under review for journal Atmos. Chem. Phys.
Published: 15 December 2016

Atmospheric Chemistry and Physics Discussions

liquid solution. Some (e.g. Kuo et al., 2011) assumed the liquid solution forms a thin layer covering the whole grain surface while Domine et al. (2013) suggested the liquid is located in grooves at grain boundaries and triple junctions. His arguments were 1) The ionic concentration is low in natural snow that only small amount of liquid can be form; and 2) The wettability of ice is imperfect. These arguments imply the layer thickness could be less than a monolayer solution if the liquid were covering the entire grain surface, which is unrealistic.

The partitioning of trace gases between air and the liquid fraction of snow can be described by Henry's law using the effective dimensionless Henry's law coefficient, $k_{\mathrm{H}}^{\mathrm{eff}}$, according to Sander (1999)

$$k_{\mathrm{H}}^{\mathrm{eff}} = k_{\mathrm{H}}^{\mathrm{cc}} \frac{\mathrm{K_a}}{[\mathrm{H}_{(\mathrm{aq})}^{+}]} \tag{5}$$

where $k_{\mathrm{H}}^{\mathrm{cc}}$ is the dimensionless temperature dependent Henry's Law coefficient (See App. A), $\mathrm{K_a}$ is the acid dissociation constant and $[\mathrm{H}_{(\mathrm{aq})}^{+}]$ is the concentration of hydrogen ions. Fig. 1 shows the temperature and pH dependence of $k_{\mathrm{H}}^{\mathrm{eff}}$. At a given pH, the $k_{\mathrm{H}}^{\mathrm{eff}}$ at 230 K is a factor greater than 200 larger than the value at 270 K. While at a given temperature, within the range of pH in natural surface snow (5 - 6.5, Udisti et al., 2004), the values remain in the same order of magnitude.

3 Modelling Approach

Two physical exchange models, Model 1 and 2, are developed from first principles to calculate the concentration of $\mathrm{NO_3^-}$ in the skin layer of snowpack. Model constraints are the observed atmospheric $\mathrm{HNO_3}$ concentration, air temperature, skin layer snow temperature, atmospheric pressure and atmospheric humidity. For simplicity, the snow grains are assumed to be spherical and constant in morphology, i.e. snow metamorphism is not taken into account.

3.1 Model 1 - Surface Adsorption/Solvation & Solid Diffusion

Different processes are used to define the grain surface concentration depending on the temperature. The detection of the disordered layer on the outer of a pure ice surface starts between 238 and 270 K depending on the measuring technique (Domine et al., 2013 and references therein). Here, the threshold temperature, T_o, is set to the lower end of the range of observation, 238 K, such that below T_o, the grain surface is assumed to be ice and its concentration is described by the combination of non-equilibrium kinetic adsorption and co-condensation (Sect. 3.1.1 and Fig. 2a). When temperature is above T_o (= 238 K) the interfacial layer between air and snow grain is defined as 'Air-DI'. The DI concentration is specified by non-equilibrium kinetic solvation (See Sect. 3.1.2 and Fig. 2b). The concentration gradient between the surface of the grain and its centre leads to solid-state diffusion and formed solid $\mathrm{NO_3^-}$ solution (sect. 3.1.3).

Atmos. Chem. Phys. Discuss., doi:10.5194/acp-2016-1069, 2016
Manuscript under review for journal Atmos. Chem. Phys.
Published: 15 December 2016

Atmospheric Chemistry and Physics Discussions

3.1.1 Ambient Temperature $\leq$ 238 K: Non-Equilibrium Kinetic Surface Adsorption & Co-condensation

At temperatures below 238 K the interface between air and snow grain surface is assumed to be pure ice. The grain surface concentration, $[\mathrm{HNO_{3\,(surf)}}]$, is determined by a combination of non-equilibrium kinetic adsorption and co-condensation:

$$[\mathrm{HNO_{3\,(surf)}}] = [\mathrm{HNO_{3\,(ads)}}] + [\mathrm{HNO_{3\,(cc)}}] \qquad \text{if} \quad T \leq 238\mathrm{K} \tag{6}$$

where $[\mathrm{HNO_{3\,(ads)}}]$ is the concentration contributed from surface adsorption and $[\mathrm{HNO_{3\,(cc)}}]$ is the concentration contributed from co-condensation.

A non-equilibrium kinetic approach is taken instead of saturation or equilibrium adsorption for three main reasons: Ullerstam et al. (2005b) have shown that for partial pressures of $\mathrm{HNO_3}$ lower than 10^{-5} Pa the ice surface is not entirely covered and therefore undersaturated. The annual average atmospheric partial pressure of $\mathrm{HNO_3}$ recorded at Dome C is $\sim 10^{-6}$ Pa (Traversi et al., 2014) and is $\sim 10^{-7}$ Pa at Halley (Jones et al., 2008), hence, the ice surface is unlikely to be saturated with $\mathrm{HNO_3}$. Secondly, natural snowpacks are constantly undergoing sublimation and condensation of $\mathrm{H_2O}$, especially at the skin layer, due to temperature gradient over a range of timescales from fraction of seconds to diurnally and seasonally (Bartels-Rausch et al., 2014). Pinzer et al. (2012) observed up to 60% of the total ice mass redistributed under a constant temperature gradient of 50 $\mathrm{K\,m^{-1}}$ over a 12 hour period. In Dome C, the modelled (See Sect. 4) mean absolute temperature gradient across the top 4 mm of the snowpack was 130 $\mathrm{K\,m^{-1}}$ in summer and 98 $\mathrm{K\,m^{-1}}$ in winter and at Halley, the mean absolute temperature gradient across the top 10 mm was around 41 and 34 $\mathrm{K\,m^{-1}}$ in the summer and winter period respectively. Therefore, the grain surface has a dynamic character of which 'fresh' grain surface would be created by 'new' water molecules before equilibrium can be reached between air and surface of the snow grain. Lastly, as mentioned in the Introduction, at the average temperature range found in Antarctica (0°−-60°C) the characteristic time of surface adsorption is on the order of 10^2-10^3 s, which is longer than the model time resolution (10 min).

The net rate of adsorption can be described as $\frac{d\mathrm{HNO_3}}{dt} = k_{\mathrm{ads}}[\mathrm{HNO_{3\,(g)}}]\,[\mathrm{S}] - k_{\mathrm{des}}[\mathrm{HNO_{3\,(ads)}}]$. Substituting k_{ads} with Eq. (3), the net adsorption rate is expressed as

$$\frac{d[\mathrm{HNO_{3\,(ads)}}]}{dt} = k_{\mathrm{ads}}\left([\mathrm{HNO_{3\,(g)}}]\,[\mathrm{S}] - \frac{[\mathrm{HNO_{3\,(ads)}}]}{K_{\mathrm{eq}}}\right) \tag{7}$$

The temperature gradient and relative humidity gradient between the surface of the snowpack and the skin layer create a gradient in water vapour pressure, which drives condensation or sublimation of snow, depending on the sign of the gradient. During the condensation process the adsorbed molecules may bury in the growing ice if its residence time on the surface is long enough compare to the frequency of water molecules hitting the grain surface (Bartels-Rausch et al., 2014). Uptake of $\mathrm{HNO_3}$ molecules to growing ice is known as co-condensation. The surface $\mathrm{NO_3^-}$ concentration

Atmos. Chem. Phys. Discuss., doi:10.5194/acp-2016-1069, 2016
Manuscript under review for journal Atmos. Chem. Phys.
Published: 15 December 2016

Atmospheric Chemistry and Physics Discussions

contributed by co-condensation, $[\mathrm{HNO_{3\,(cc)}}]$, is given by

$$[\mathrm{HNO_{3(cc)}}] = X_{\mathrm{HNO_3}} \frac{\rho_{ice} N_A}{\overline{m}_{\mathrm{H_2O}}} \frac{\Delta t}{\mathrm{V_{grain}}} \frac{d\mathrm{V}}{dt} \tag{8}$$

where $\mathrm{X_{HNO_3}}$ is the mole fraction of $\mathrm{HNO_3}$ condensed along with water vapour ($\mathrm{X_{HNO_3}} = \frac{P^{0.56}_{\mathrm{HNO_3}}}{10^{3.2}}$, Ullerstam and Abbatt, 2005a), ρ_{ice} is the density of ice (in $\mathrm{kg\,m^{-3}}$), N_A is the Avogadro's constant (6.022×10^{23} $\mathrm{molecule\,mol^{-1}}$) and Δt is the model time step. The rate of volume change of snow grain, $\frac{dV}{dt}$, is specified by the growth law by described (Flanner and Zender, 2006)

$$\frac{d\mathrm{V}}{dt} = \frac{4\,\pi\,\mathrm{R_{eff}}}{\rho_{ice}} D_v \left(\frac{d\,\rho_v}{d\,z}\right)_{z=r} \tag{9}$$

where $\mathrm{R_{eff}}$ is the effective radius, D_v is the diffusivity of water vapour in air and $\frac{d\,\rho_v}{d\,z}$ is the local water vapour density gradient, i.e. between air away from the snow grain and the air near the grain surface. However, to the author's knowledge there are no observations reported and the calculation of water vapour density at these microscopic scales is computational costly as it would require 3-D modelling of the metamorphism of the snow grain. For simplicity the macroscopic (few mm) water vapour gradient across the skin layer was used to estimate the condensation and sublimation processes. The water vapour density, ρ_v,is defined as follows:

$$\rho_v = \frac{P_{sat}\,\mathrm{RH}}{100\,R_v\,T} \tag{10}$$

where P_{sat} is the saturated vapour pressure (Pa), RH is the relative humidity (%), R_v is the gas constant of water vapour ($\mathrm{J\,kg^{-1}\,K^{-1}}$) and T is temperature (K). There are no measurement of fine resolution of vertical snow profile of RH and temperature available, therefore, RH within the snowpack was assumed to be 100% and the temperature of the skin layer is estimated using a heat transfer temperature model (Hutterli et al., 2003) of which based on the heat diffusion equation:

$$\frac{\partial T}{\partial t} = \frac{\partial}{\partial z} k_w(z) \frac{\partial T}{\partial z} \tag{11}$$

where T is the temperature, t is time, k_w is the heat conductivity and z is the depth.

3.1.2 Ambient Temperature > 238 K: Non-Equilibrium Solvation

At temperatures above 238 K, the interface between air and snow grain surface is assumed to be a DI, with characteristics described in the Introduction. The grain surface concentration is determined by non-equilibrium solvation in the DI, which covers the entire grain surface.

$$[\mathrm{HNO_{3\,(surf)}}] = [\mathrm{HNO_{3\,(DI)}}] \qquad \text{if} \quad T > 238\mathrm{K} \tag{12}$$

The DI is also assumed to be out of equilibrium with the surrounding air as discussed above. The surface concentration is then defined by the following equation:

$$\frac{d[\mathrm{HNO_{3\,(DI)}}]}{dt} = k_{\mathrm{mt}} \left([\mathrm{HNO_{3\,(g)}}] - \frac{[\mathrm{HNO_{3\,(DI)}}]}{k^{\mathrm{eff}}_{\mathrm{H}}}\right) \tag{13}$$

Atmos. Chem. Phys. Discuss., doi:10.5194/acp-2016-1069, 2016
Manuscript under review for journal Atmos. Chem. Phys.
Published: 15 December 2016

Atmospheric Chemistry and Physics Discussions

The mass-transfer coefficient, $k_{\mathrm{mt}} = \left(\frac{\mathrm{R_{eff}}^2}{3\,D_g} + \frac{4\,\mathrm{R_{eff}}}{3\,\overline{v}\,\alpha}\right)^{-1}$, where D_g is the gas-phase diffusivity (Sander, 1999).

3.1.3 Solid Diffusion

In this model radially symmetrical spherical grains with a radius, $\mathrm{R_{eff}}$, are assumed and the radius is determined from snow specific surface area (SSA) measurements, as follows:

$$\mathrm{R_{eff}} = \frac{3}{\rho_{\mathrm{ice}}\,\mathrm{SSA}} \tag{14}$$

where ρ_{ice} is the density of ice. The concentration gradient of $\mathrm{NO_3^-}$ between the surface and the centre of the snow grain causes solid state diffusion of nitric acid. The nitric acid forms a solid solution with ice. The grain surface concentration is defined by either adsorption and co-condensation on ice (sect. 3.1.1) or solvation in the DI (sect. 3.1.2) as a function of temperature. The spherical solid-state diffusion equation is given by

$$\frac{\partial[\mathrm{NO_3^-}](r)}{\partial t} = k_{\mathrm{diff}}\left(\frac{2}{r}\frac{\partial[\mathrm{NO_3^-}](r)}{\partial r} + \frac{\partial^2[\mathrm{NO_3^-}](r)}{\partial r^2}\right) \tag{15}$$

where $[\mathrm{NO_3^-}](r)$ is the local $\mathrm{NO_3^-}$ concentration in the r^{th} layer of the ice sphere and k_{diff} is the diffusion coefficient in the solid-phase for ice. The typical length-scale of the molecule diffuses in a given time, t, can be described by the root-mean square displacement, $<x> = \sqrt{6tk_{\mathrm{diff}}}$. The characteristic distance x during one model time step of Δt = 10 min is 1.5 and 5.5 μm at Dome C (Sect. 4.1) and Halley (Sect. 4.2), respectively. To optimise the performance and computational cost of the models, 85 evenly spread concentric shells (i.e. r = 1, 2, 3, ..., 85 with 85^{th} being the outermost shell) were assumed, such that the average thickness of the concentric shell is less than the average root-mean square displacement.

The diffusion equation is solved with the Crank Nicolson scheme (Press et al., 1996) and the bulk $\mathrm{NO_3^-}$ concentration, $[\mathrm{NO^-_{3(bulk)}}]$, is the sum of the number of $\mathrm{NO_3^-}$ in each layer divided by the volume of the grain, expressed as

$$[\mathrm{NO^-_{3(bulk)}}] = \frac{\sum[\mathrm{NO_3^-}](r)\,V(r)}{\sum V(r)} \tag{16}$$

where $V(r)$ is the volume of the r^{th} layer and $\sum V(r)$ is the total volume of the grain, V_{grain}.

3.2 Model 2 - Non-Equilibrium Kinetic Adsorption & Solid Diffusion + Equilibrium Air - Micro-Liquid Pocket

Model 2 (Schematic in Fig. 3) is based on the hypothesis that at all temperature below melting, T_m the majority of the grain surface is ice and liquid is presented above the eutectic temperature, T_e, which is in the form of micropocket and located in grooves at grain boundaries and triple junctions

Atmos. Chem. Phys. Discuss., doi:10.5194/acp-2016-1069, 2016
Manuscript under review for journal Atmos. Chem. Phys.
Published: 15 December 2016

Atmospheric Chemistry and Physics Discussions

(Domine et al., 2013). The bulk NO_3^- concentration in Model 2 is defined as follow:

$$[NO^-_{3\,(\mathrm{bulk})}] = \begin{cases} \frac{\sum [NO_3^-](r)\,V(r)}{V_{\mathrm{grain}}} & \text{if} \quad T < T_e. \\ \frac{\sum [NO_3^-](r)\,V(r)}{V_{\mathrm{grain}}} + \phi_{H_2O}\, k_H^{\mathrm{eff}}\, [HNO_{3\,(g)}] & \text{if} \quad T_e \leq T < T_m. \end{cases} \tag{17}$$

At all temperatures below T_m, HNO_3 could be adsorbed on, co-condensed to or co-sublimated from the surface (Same description as in Sect. 3.1.1). The adsorbed molecules on the grain surface can then be diffused into or out of the bulk ice depending on the concentration gradient of NO_3^- between the grain surface and the grain core (Same description as in 3.1.3). Above T_e, liquid co-exists with ice (Last term in Eq. 17, if $T_e \leq T < T_m$). The volume of the micropocket is calculated from the liquid water fraction, ϕ_{H_2O}, by Eq. 4. The partitioning between air and the micropocket is described by Henry's Law, with the effective Henry's Law coefficient, k_H^{eff}, as the partitioning coefficient. An instantaneous equilibrium is assumed because 1) the volume of the liquid solution is small ($10^{-7} - 10^{-6}\%$ of the total volume of the ice grain, discussed below); 2) HNO_3 is highly soluble in water; and 3) the diffusion rate is faster in liquid (At 0°C, NO_3^- diffusion of NO_3^- is $9.78 \times 10^{-10}\ \mathrm{m^2\,s^{-1}}$ in liquid, Yuan-Hui and Gregory, 1974) than in ice (At 0°C NO_3^- diffusion rate is $3.8 \times 10^{-14}\ \mathrm{m^2\,s^{-1}}$ in ice). The exact location of the micropockets are not specified in the model and it is considered as a droplet on the surface. However, the volume of the micropocket is so small the grain surface covered by the liquid is assumed to be negligible.

Both the values of pH and $\Phi^{\mathrm{aq}}_{\mathrm{bulk}}$ are updated at each time step with the hydrogen ion concentration and total ionic concentration from previous time step. At Dome C, the major anion in melted snow is NO_3^- (e.g. Udisti et al., 2004). It is assumed that the nitrate and hydrogen ions are the only ions presented in the skin layer snow, i.e. $[\mathrm{Ion}_{\mathrm{tot\,(bulk)}}] = 2\times[NO_3^-]$ in Eq. 4, and the eutectic temperature of the H_2O-HNO_3 system 230.64 K (Beyer et al., 2002) is chosen as the threshold temperature for the existence of micropocket. In contrast, at Halley snowpack ion chemistry is dominated by $NaCl$ (Wolff et al., 2008), contributing ~85% of the total ionic concentration in the 2004-05 Halley data set, due to the proximity of sea ice and open ocean. For simplicity, the only anions concentration included in the calculation of ϕ_{H_2O} are NO_3^- and Cl^-, such that $[\mathrm{Ion}_{\mathrm{tot\,(bulk)}}] = 2\times([Cl^-] + [NO_3^-])$ in Eq. 4 and T_e used is that for a H_2O-$NaCl$ system 251.95 K (Akinfiev et al., 2001).

4 Model Validation

Atmospheric nitrate, skin layer snow NO_3^- concentration, meteorological data and information were collected at Dome C ($75°06'S, 123°33'E$) from January 2009 to January 2010 and Halley ($75°35'S, 26°39'E$) between April 2004 and February 2005, Antarctica.

4.1 Observation at Dome C

Dome C is chosen as 1) All year temperatures are below freezing and no snow melt occurs, the mean annual temperature (e.g. Argentini et al., 2014) is around $-52°C$ with maximum temperature of

Atmos. Chem. Phys. Discuss., doi:10.5194/acp-2016-1069, 2016
Manuscript under review for journal Atmos. Chem. Phys.
Published: 15 December 2016

Atmospheric Chemistry and Physics Discussions

$-17°C$ in summer (mid November till end of January) and down to $-80°C$ in the winter (April to mid September). The diurnal temperature variation is approximately 10 K in summer, spring (mid September till mid November) and autumn (beginning of February till end of March) period. 2) Relatively simple snow nitrogen chemistry. The concentration of sea salt and other organic particles that scavenge HNO_3 are low in East Antarctica Plateau (Legrand et al., 2016). Hence, the main source of NO_3^- in snow is atmospheric HNO_3 that dissolved in and/or adsorbed onto the grain (Traversi et al., 2014). 3) Low accumulation rate of snow of 27 $kg\,m^{-2}\,yr^{-1}$ (Röthlisberger et al., 2000), implies strong post-depositional processing of nitrate before the surface snow get buried by fresh snowfall (e.g. Röthlisberger et al., 2000; Frey et al., 2009).

The temperature, atmospheric pressure, atmospheric nitrate and skin layer snow nitrate concentration measured during January 2009 to 2010 at Dome C (published perviously by Erbland et al., 2013, Fig. 6) are shown in Fig. 4. The atmospheric nitrate, the sum of atmospheric particulate nitrate ($p-NO_3^-$) and gaseous nitric acid (HNO_3), was collected on glass fibre filter by high volume air sampler (HVAS) as described in Morin et al. (2008). The filter was positioned approximately 1 m above the snow surface and was being changed on a weekly base. Erbland et al. (2013) stated that the particulate nitrate data shows good agreement with HNO_3 gas-phase concentration measured by denuder tubes at Dome C over the same time period, therefore we equate the observed atmospheric nitrate with gaseous HNO_3. Maximum atmospheric HNO_3 of 167 $ng\,m^{-3}$ was observed during summer period, while minimum concentration of 1.2 $ng\,m^{-3}$ was recorded during autumn and early winter period. The snow samples were collected from the 'skin layer' snow, the top 4 ± 2 mm of the snowpack, approximately every 3 days. The skin layer was assumed to be spatially heterogeneous with an uncertainty in thickness about 20% due to the softness of the uppermost layer and sampling from different people. The nitrate concentration in the melted sample was measured by ion chromatograph (IC).

Continuous meteorological observation and snow science are carried out at Dome C under the 'Routine Meteorological Observations' of the Concordia Project by the Italian National Antarctic Research Programme, PNRA, and the French Polar Institute, IPEV (http://www.climantartide.it). Here are the brief informations of the meteorological observations, details of the methodology on meteorological data collection at Dome C can be found in the URL link above. Wind, temperature and moisture were measured with10 s resolution, and archived as the hourly mean. The sensor for wind speed (optoelectronic counter, WAA 15A) and direction (anemometer, WAV 15A) were mounted at 3.3 m above the snow with accuracy 0.3 $m\,s^{-1}$ and 2.8 ° respectively. Temperature and relative humidity were measured at 1.6 m above the snow surface by a platinum resistance thermometer, VAISALA PT100 DTS12, with precision of $\pm$ 0.13 °C at -15 °C, and the humidity sensor was a HUMICAP by VAISALA with a precision of $\pm$ 2 %. Atmospheric nitrate concentrations and meteorological data have been interpolated into 10 minute resolution as model input.

Atmos. Chem. Phys. Discuss., doi:10.5194/acp-2016-1069, 2016
Manuscript under review for journal Atmos. Chem. Phys.
Published: 15 December 2016

Atmospheric Chemistry and Physics Discussions

There are no available pH measurements of the snowpack, therefore, the pH of the DI in Model 1 and the initial pH in Model 2 is assumed to be 5.6 (Udisti et al., 2004). Picard et al. (2016) shows the SSA of the near-surface snow during winter months are significantly larger than SSA in the summer months, hence, a single value of SSA is not representative and sufficient enough for a year-long model run. There are no SSA recorded during 2009-2010 for skin layer snow and the SSA is estimated base on observation at Dome C from 2012 to 2015 by Picard et al. (2016), as shown in Fig. 5 (solid black line).

4.2 Observation at Halley

Halley is at a similar latitude to Dome C but at sea level in coastal Antarctica with very different geographic features. Halley is sitting on the Brunt Ice Shelf and is close to the Weddell Sea in three directions. Hence, both the temperature and humidity are very different from Dome C and its atmospheric composition is more complex due to the larger influence by different aerosols such as sea salt and dust aerosols. The average surface temperature in summer days is around $-10^{\circ}\mathrm{C}$ and below $-20^{\circ}\mathrm{C}$ in the winter. Being a coastal site, occasionally, temperature can rise above $0^{\circ}\mathrm{C}$ (surface melt is possible) or drop to $-55^{\circ}\mathrm{C}$. The snow accumulation rate at Halley is much larger compared to Dome C, which have an average of 112 $\mathrm{kg\,m^{-2}\,yr^{-1}}$ (Arthern et al., 2006).

Meteorological and chemical data were collected at Halley under the CHABLIS (Chemistry of the Antarctic Boundary Layer and the Interface with Snow) campaign at the Clean Air Sector Laboratory (CASLab). Details of the methodology of the measurements can be found in Jones et al. (2008) and Jones et al. (2011). Measurement of atmospheric $\mathrm{HNO_3}$ concentrations were carried out at weekly resolution using annular denuders (URG corporation) mounted at 7-8 m above the snow surface with a collection efficiency of 91% during CHABLIS (Jones et al., 2008). Surface snow (the top 10 to 25 mm) was collected on a daily basis and the samples were analysed using ion chromatography (IC). Bulk concentrations of the major anions and cations were measured, including $\mathrm{Cl^-}$ and $\mathrm{NO_3^-}$. The concentrations were interpolated to the 10 minutes model resolution.

Other meteorological data including 10 minute averages of air temperature by Aspirated PRT, RH by Humidity probe (Vaisala Corp) and wind speed and direction by Propeller vane, all sensors were at 1 m above snow surface. The data from Halley collected during CHABLIS are shown in Fig. 6. Daily values were interpolated to the model time step of 10 min. No observations of SSA are available for Halley. Therefore the observation of SSA from Dome C were adjusted taking into account of the shorter cold period, which tend to have a larger SSA (i.e. smaller grain size, Eq. 14).

4.3 Statistical Analysis

Three-day running means are calculated from all model outputs to match the average time resolution of the observations. The performance of the models are assessed by the coefficient of variation of

Atmos. Chem. Phys. Discuss., doi:10.5194/acp-2016-1069, 2016
Manuscript under review for journal Atmos. Chem. Phys.
Published: 15 December 2016

Atmospheric Chemistry and Physics Discussions

RMSE, $C_v(\mathrm{RMSE})$, defined as

$$C_v(\mathrm{RMSE}) = \frac{\sqrt{\sum_{t=1}^{n}(obs(t) - model(t))^2 / n}}{\overline{obs}} \quad (18)$$

where $obs(t)$ and $model(t)$ the observed value and modelled value at time t, n is the number of observation points, and $\overline{obs}$ is the observation mean.

5 Results

Below we describe the results from Model 1 and 2 at Dome C and Halley. Model fits for observations are assessed by $C_v(\mathrm{RMSE})$ and summarised in Table 2 and 3.

5.1 Dome C

The modelled results from Model 1 - 'Surface Adsorption/Solvation & Solid Diffusion' are shown in Fig. 7 and results from Model 2 - 'Surface Adsorption & Solid Diffusion + micropocket' is presented in Fig. 8. Both models are temperature dependent, therefore, the results will be presented by season.

5.1.1 Winter

The average temperature ($\pm 1\sigma$) at Dome C between late autumn to late spring in 2009 is 213.7($\pm$7.9) K (Fig. 4), which is lower than the threshold temperature for detection of DI layer (set at 238 K) within Model 1 and lower than eutectic temperature for a H_2O-HNO_3 mixture (230 K) within Model 2. Therefore, during winter, the dominant controlling mechanisms are the combination of non-equilibrium kinetic surface adsorption and co-condensation coupled to solid state diffusion within the snow grain for both models. The combination of these two processes agreed very well with the observations, such as the small peak from mid April to early May and from mid to end of August, followed by a tough and then a steady increase from middle September to end of October, apart from one peak in late February (Fig. 7).

As mentioned in Introduction, Bock et al. (2016) suggested during the winter months the skin layer snow nitrate concentration is driven by thermodynamic equilibrium ice solubility in ice followed by solid-state diffusion instead (Configuration 2 - BC1 within Bock et al., 2016, and is referring as the 'Equilibrium' approach hereon). The grain surface concentration, $[HNO_{3\,(surf)}]$, for the 'Equilibrium' approach is determined by parameterisation from Thibert et al. (1998):

$$[HNO_{3\,(surf)}] = 2.37 \times 10^{-12} \exp\left(\frac{3532.2}{T}\right) P_{HNO_3}^{1/2.3} \frac{\rho_{ice} N_A}{MM_{H2O}} \quad (19)$$

where T is the snow temperature (K), P_{HNO_3} is the partial pressure of HNO_3 (Pa). To compare the two different approaches for estimating skin layer $[NO_3^-]$ in the winter period, the 'Equilibrium Approach' was run along with an 'non-equilibrium kinetic surface adsorption followed by solid diffusion' configuration (referring as the 'Kinetic' approach hereon). Note that the co-condensation

Atmos. Chem. Phys. Discuss., doi:10.5194/acp-2016-1069, 2016
Manuscript under review for journal Atmos. Chem. Phys.
Published: 15 December 2016

Atmospheric Chemistry and Physics Discussions

was excluded in these model runs for a direct comparison between the two different approaches. Both the 'Equilibrium' and 'Kinetic' Approach resulted a very similar trend and variation until mid Sept (Fig. 9, Left). Despite the 'Kinetic' approach yielding a larger $C_v(\mathrm{RMSE})$ compared to the 'Equilibrium' approach, the 'Kinetic' approach appears to capture the temporal patten from mid September till early November, yet, the 'Equilibrium' approach does not.

5.1.2 Summer

The average temperature ($\pm 1\sigma$) in late spring, summer and early autumn is 240.0($\pm$5.0) K and so the main controlling process is the solvation in DI in Model 1 and partitioning in the micropocket in Model 2.

In Model 1 the solvation of NO_3^- in DI followed by solid-state diffusion captured some trends observed in early spring and during the summer period (Fig. 7), including the decrease from the beginning of February, the rise between mid and late November, the sharp increase in mid December. It also reproduced the steep decrease in concentration at the beginning of 2010. However, Model 1 did not capture the peak in early February and overestimated concentration by a factor of 1.5-5 in December.

The results from Model 2 was reasonably well agreed with the observation in these few months with $C_v(\mathrm{RMSE})$ of 0.6703. The decrease in concentration at beginning of February was captured with the additional partitioning of HNO_3 in micropocket so as other trends such as the rise and dip in November and from mid December till January next year (Fig. 8). The modelled bulk NO_3^- concentrations in the summer were also the same order of magnitude yet either over or underestimated by a factor of 3, that of observations.

5.2 Halley

The modelled results from Model 1 - 'Surface Adsorption/Solvation & Solid Diffusion' are shown in Fig. 10 and results from Model 2 - 'Surface Adsorption & Solid Diffusion + micropocket' are presented in Fig. 11. As in Sect. 5.1, results will be presented by the season. Halley is located at sea level and is influenced by atmospheric advection of moist air so that spring and early autumn are significantly warmer than winter compared to Dome C. The $C_v(\mathrm{RMSE})$ values for different modelled results are shown in Table 3.

5.2.1 Late Autumn to Winter

The mean temperature ($\pm 1\sigma$) during this period at Halley is 244.72($\pm$7.7) K, which is higher than the threshold temperature for detection of DI layer majority of the time but lower than the eutectic temperature for a H_2O-NaCl mixture (251 K). Therefore, the main controlling process is solvation in DI in Model 1 whereas in Model 2 the main controlling processes are the combination of non-equilibrium adsorption and co-condensation coupled with solid-state diffusion. Performance of

Atmos. Chem. Phys. Discuss., doi:10.5194/acp-2016-1069, 2016
Manuscript under review for journal Atmos. Chem. Phys.
Published: 15 December 2016

Atmospheric Chemistry and Physics Discussions

Model 1 was poor ($C_v(RMSE)$ = 27.78), it has overestimated the NO_3^- concentration by an order of magnitude (Fig. 10). However, few of the trends were reproduced during this cold period such as the two small peaks in mid April and early May and the rise in mid September.

The modelled results from Model 2 were much closer match to the observation compared to Model 1 ($C_v(RMSE)$ = 1.08). It has captured the first peak in mid April, the steady rise in July and the small peak in beginning of September. However, it did not reproduce the sharp peak in mid August and underestimated the NO_3^- concentration for the majority of the time.

Similar to the Dome C site, the 'Equilibrium' approach after Bock et al. (2016) was run alongside the 'Kinetic' approach from late autumn until winter, again, no co-condensation processes were included in these 2 runs for a direct comparison. The modelled results from both approaches are very similar in value and temporal variations (Fig. 9, Right). Again, both the 'Kinetic' and 'Equilibrium' approach failed to reproduce the sharp peak in mid August.

5.2.2 Spring - Summer - Early Autumn

Similar to the winter months, Model 1 overestimated the bulk NO_3^- concentration at Halley by an order of magnitude and failed to capture any of the variability (Fig. 10). Model 2, however, reproduced some features during the warmer months, such as the peak in late September followed by a steady rise in October, the spikes in mid December, beginning of and mid January and also the peak and trough in late January (Fig. 11). The modelled results are within the same order of magnitude and obtained a $C_v(RMSE)$ of 0.6510.

6 Discussion

The model results from both Model 1 and 2 show that the bulk NO_3^- concentration in surface snow can be reasonably well described by physical non-equilibrium adsorption and co-condensation coupled with solid-state diffusion during autumn to spring at Dome C and in winter at Halley, i.e. when it is cold and the solar irradiance is small. In the summer months, the combination of larger temperatures and a larger diurnal temperature range causes the 'Air-Ice' only processes to no longer provide an accurate prediction. For the majority of this period, the NO_3^- concentration in surface snow is governed by solvation in DI in Model 1 or partitioning in micropocket in Model 2.

Model 1 matches reasonably well the year-round observations at Dome C ($C_v(RMSE)$ = 1.34), yet, it overestimates those at Halley by an order of magnitude ($C_v(RMSE)$ = 89.28). On the other hand, results from Model 2 agree well for both study sites all year-round ($C_v(RMSE)$ = 0.84 for both Dome C and Halley). Generally, the mismatch between the models and observations can be separated into 2 categories - data limitations and model configurations, and will be discussed below.

Firstly, the temporal resolution of atmospheric nitrate concentration data at both study sites were roughly 5 to 10 days, therefore, any substantial changes in the atmospheric input within a short time

Atmos. Chem. Phys. Discuss., doi:10.5194/acp-2016-1069, 2016
Manuscript under review for journal Atmos. Chem. Phys.
Published: 15 December 2016

Atmospheric Chemistry and Physics Discussions

scale might be missed and consequently the relative changes in nitrate snow concentration might not be detected. Secondly, the vertical snow pit profile of NO_3^- in Antarctica tends to have a maximum concentration in the surface snow (Röthlisberger et al., 2000), especially during the summer period, and the concentration of snow NO_3^- decreases sharply with depth. It is this thin layer of surface snow that had most post-depositional influence by the atmospheric nitrate. The Dome C snow samples were collected carefully from the top 4 ± 2 mm while the snow samples from Halley were collected from the near-surface snow (top 0 to 25 mm). It is possible that the snow NO_3^- concentration measured from Halley might be 'diluted' from deeper snow layer and does not fully represent the interaction between the thin layer on the surface of the snowpack and the overlying atmosphere. Hence, the model might appears to be 'overestimating' the $[NO_3^-]$ due to this dilution. Thirdly, atmospheric nitrate can be in the labile form of nitric acid (HNO_3) or fixed by sea salt, ammonium or terrestrial dust, therefore, the assumption of HNO_3 concentration to be equal to the total measured atmospheric nitrate might cause mismatch between the modelled and observation. Atmospheric sea salt aerosol concentrations have strong seasonal variability at Dome C. The maximum sea-salt aerosol concentration tends to be in late winter/early spring and can be up to 4 times larger than the annual mean (Legrand et al., 2016). The increase in sea salt concentration decreases the ratio of concentration of gaseous HNO_3 to total atmospheric nitrate. A possible explanation for the overestimation of NO_3^- concentration in both Model 1 and 2 in November at Dome C. Last but not least, information on precipitation, such as occurrence of new snowfall and the nitrate concentration of fresh snow, were incomplete for both datasets. Single snowfall can increase the nitrate concentration by up to factor of 4 higher than the surrounding background (Wolff et al., 2008). The contribution from fresh precipitation might not be as influential at the low accumulation site, like Dome C - 27 $kg\,m^{-2}\,yr^{-1}$ (Röthlisberger et al., 2000), compare to site with high accumulation like Halley $\sim$112 $kg\,m^{-2}\,yr^{-1}$ (Arthern et al., 2006). Wolff et al. (2008) reports that the large bulk NO_3^- concentration recorded from mid till end of August is corresponded to new snowfall, which explained why it is not captured by both models. In the following sections, the specific processes included within the two models presented in this paper will be discussed.

6.1 'Kinetic' Approach vs 'Equilibrium' Approach

The 'Kinetic' approach defines the ice surface concentration by non-equilibrium kinetic surface adsorption while the 'Equilibrium' approach after Bock et al. (2016) defines the ice surface concentration by thermodynamic equilibrium ice solubility. Both approaches are used to describe the interaction between air and ice, therefore, only results from the winter period are compared. For both sites, the 'Kinetic' and 'Equilibrium' approach resulted very similar trends except the peak in late October at Dome C (Fig. 9), of which the 'Kinetic' approach managed to capture but not the 'Equilibrium' approach. The late October $[NO_3^-]$ peak at Dome C is corresponded to the increase in

Atmos. Chem. Phys. Discuss., doi:10.5194/acp-2016-1069, 2016
Manuscript under review for journal Atmos. Chem. Phys.
Published: 15 December 2016

Atmospheric Chemistry and Physics Discussions

atmospheric nitrate (Fig. 4). In Bock et al. (2016), the late October peak was achieved after adding in an adjustable co-condensation parameter.

The grain surface concentration of the 'Equilibrium' approach is defined as Eq. 19 and is a function of the partial pressure of HNO_3 with an exponent of 1/2.3 while the grain surface concentration of the 'Kinetic Approach' is defined as Eq. 7 and is linearly related to the atmospheric nitrate concentration, therefore, the 'Equilibrium' approach is less responsive to changes in the atmospheric nitrate concentration compares to the 'Kinetic' approach. There are other advantages of applying a 'Kinetic' approach, 1) as it suits the dynamic character of the grain surface due to constantly changing temperature gradient. 2) as it suits sites with a high accumulation rate where the skin layer is buried by subsequent snowfall before reaching equilibrium.

At Halley, the NO_3^- concentration is underestimated by both approaches. There are 2 possible explanations. First, the SSA values used maybe underestimated and leads to an underestimation on adsorption , further field observations are required to confirm it. Secondly, it might indicate other processes might be involved in defining the snow surface concentration of NO_3^-, such as precipitation or micropocket (Sect. 6.4).

6.2 Co-Condensation - 'Air-Ice' Interaction

The process of co-condensation/sublimation is considered as part of the 'Air-Ice' interaction in both Models 1 and 2. It is driven by the difference in water vapour density across the skin layer snow and the overlying atmosphere. The water vapour density gradient depends exponentially on temperature gradient. At Dome C temperatures are extremely low, especially in winter, and therefore it is not surprising that only 2% of the grain surface concentration is contributed by co-condensation during winter and spring (Fig. 9, Left in light blue). In contrast, at Halley, where winter is warmer, ∼21% of the grain surface concentration is contributed by co-condensation during winter (Fig. 9, Left in dark blue). As shown in Table 3, the $C_v(\mathrm{RMSE})$ decreased slightly during winter after including co-condensation as part of the 'Air-Ice' interaction. In the summer, other processes are replaced (e.g. by 'Air-DI' processes in Model 1, See Sect. 6.3) or being overwhelmed (e.g. by partitioning in micropocket in Model 2, See Sect. 6.4) the co-condensation process to the overall NO_3^- concentration.

There are a few possible sources of uncertainties in the calculation of co-condensation/sublimation processes. For example, the macro-scale gradients were used instead of micro-scale gradients and there were no precise measurements of skin layer snow density. Uncertainty in the density would lead to uncertainty in the modelled skin layer snow temperature. Despite the potential errors in the calculation of co-condensation, the large NO_3^- concentration in the skin layer in the summer is unlikely due to the co-condensation process as an unrealistically high average rate of volume change, $\frac{dV}{dt}$, of 130 and 118 $\mu m^{-3}\,s^{-1}$, equivalent to an average grain volume increases of 170% and 135% everyday, would be required for Dome C and Halley respectively. Assuming the RH of skin layer snow to be 100% and RH of the overlying atmosphere is the same as measured at 1 m

Atmos. Chem. Phys. Discuss., doi:10.5194/acp-2016-1069, 2016
Manuscript under review for journal Atmos. Chem. Phys.
Published: 15 December 2016

Atmospheric Chemistry and Physics Discussions

above snowpack, a macro-temperature gradient as high as $2.7\times10^{3}\ \mathrm{K\,m^{-1}}$ would be require across the top 4 mm of the snowpack to match the large concentration of bulk $\mathrm{NO_3^-}$ in the summer at Dome C and in an average temperature gradient of 500 $\mathrm{K\,m^{-1}}$ would be require across the top 10 mm of the snowpack in Halley, which are 1- 2 orders of magnitude higher than the averaged modelled temperature gradient (listed in Sect. 3.1.1).

6.3 Disordered Interface - Model 1 (Temperature $>$ 238 K)

In Model 1, the interfacial layer between air and snow grain is described as 'Air-DI' when the ambient temperature is warmer than 238 K. At Dome C, the 'Air-DI' regime is only applicable during summer months due to the extreme cold temperatures, yet, at Halley for the majority of the time the interface is considered as 'Air-ID'. It is clear that having an 'Air-ID' interface above 238 K resulted in large all year round overestimation of bulk $\mathrm{NO_3^-}$ concentration at Halley and the overestimation of the $\mathrm{NO_3^-}$ concentration peak in early December at Dome C. The temperature threshold of 238 K was chosen as it is the lowest detection temperature for 'liquid-liker' properties in pure ice (Domine et al., 2013). However, the onset temperature of the DI on pure ice varies with different experimental setups, such as probing techniques and how the samples were prepared, the detecting temperature is ranging from 198 to 268 K (as discussed by Bartels-Rausch et al., 2014). Simulation by Conde et al. (2008) found the DI begins at 100 K below the melting point, of the particular mixture of $\mathrm{H_2O}$ and impurities, of which a small fraction of water molecules leaving the outermost crystalline layer and becoming mobile. Increasing the temperature up to 10 K below the melting point, the number of mobile $\mathrm{H_2O}$ or $\mathrm{HNO_3}$ molecules increase on the outermost crystalline layer and above that temperature the disorder might extend to an additional ice layer. The appearance and thickness of DI not only depends on temperature, but also the speciation and quantity of impurities present within the snow grain (McNeill et al., 2012). Different impurities have different impacts on the hydrogen bonding network at the ice surface and hence have different impact on the characteristics, such as thickness, of the DI (Bartels-Rausch et al., 2014). Some studies suggest that in the presence of impurities, a thick ion-containing disorder region would coexist with a region of pure ice with thin DI layer instead of a homogenous uniform DI across the whole grain surface (Sazaki et al., 2012). In order to identify the sensitivity of Model 1 to the threshold temperature, T_o, details and results of the sensitivity test is presented in the following section.

Other major assumptions made in Model 1 is the partition coefficient, the effective Henry's coefficient and the mass transport coefficient, k_{mt}, in the DI. The values were the same as those in the liquid aqueous phase and might not be realistic and lead to overestimation of solvation of $\mathrm{HNO_3}$ in the DI. However, the real values for partition and mass transport coefficients are difficult to measure with the current measurement techniques and need to be re-examined in the future. The sensitivity of Model 1 to the value of pH in the DI, hence the effective Henry's coefficient, is presented in the following section.

Atmos. Chem. Phys. Discuss., doi:10.5194/acp-2016-1069, 2016
Manuscript under review for journal Atmos. Chem. Phys.
Published: 15 December 2016

Atmospheric Chemistry and Physics Discussions

There are 2 possible explanations for why Model 1 provided a reasonable estimation for HNO_3 at Dome C, but not Halley. First, the chemical composition of surface snow in Dome C is relative simple, dominated by nitrate anion, which would induce insignificant changes to the hydrogen bonding network at the DI surface (Bartels-Rausch et al., 2014). Compared to surface snow at Halley and that its properties would be more similar to pure ice. Secondly, temperature at Halley occasionally rises above 0 °C potentially causing melting and significant changes in snow grain morphology.

6.3.1 Sensitivity Study

The work presented highlighted that the Model 1 is sensitive to the threshold temperature, T_o, but not the pH of the DI layer. In order to investigate the model sensitivity to T_o, Model 1 was evaluated by varying T_o with ΔT = 2 K up till 242 K and pH range 5.2-6.4 with $\Delta pH = \pm 0.4$. Having a slightly larger threshold temperature smoothed out some of the sharp peaks in the modelled results in the summer period at Dome C (Fig. 7, in Purple). At Halley, despite the improvement in $C_v(\mathrm{RMSE})$ when a higher temperature threshold was used, the modelled $[NO_3^-]$ is still an order of magnitude larger than the observation (Fig. 10, in Purple).

The exponential dependency of the effective Henry's law on the inverse of temperature is responsible for the sensitivity of the threshold temperature for Model 1. The solvation of HNO_3 increases as temperature decreases (Fig. 1). Having a lower threshold temperature implies including some larger surface nitrate concentration in the DI which leads to greater concentration gradient across the grain and hence larger bulk NO_3^- concentration.

Varying the pH value of the DI layer between the range of 5.2-6.4 does not have significant changes (all resulted the same $C_v(\mathrm{RMSE})$, not shown) to the estimated bulk NO_3^- concentration. The effective Henry's law coefficient found within this range of pH are in the same order of magnitude (Fig. 1).

6.4 Micro-Liquid Pocket - Model 2 (Temperature > Eutectic Temperature)

Model 2, with the liquid micropocket and non-equilibrium surface adsorption and co-condensation coupled with solid diffusion within the grain, managed to replicate the bulk NO_3^- concentration of the surface snow without any tuning parameters for both Dome C and Halley even in the summer months. In the summer, the partitioning to the micropocket contributed ∼75% and ∼80% of the total NO_3^- concentration at Dome C and Halley respectively. This is a crucial outcome as it indicated Model 2 can be used for predicting the air-snow exchange of nitrate for wide range of meteorological conditions and locations, which have impacts on the chemical composition of snow.

The over or underestimation of NO_3^- concentration by Model 2 can be explained by the simplification of nitrate only impurity at Dome C or nitrate and salt as impurity at Halley. The liquid water fraction is a function of total ionic concentration (See Eq. 4), neglecting the existence of other ions might lead to underestimation of micropocket volume. The additional liquid would increase

Atmos. Chem. Phys. Discuss., doi:10.5194/acp-2016-1069, 2016
Manuscript under review for journal Atmos. Chem. Phys.
Published: 15 December 2016

Atmospheric Chemistry and Physics Discussions

the dissolution capacity for HNO_3 and hence increase the estimated NO_3^- concentration. As shown in Fig. 11, the estimated bulk NO_3^- concentration followed a similar trend as the measured ionic concentration, which was simplified (See Sect. 3.2).

Nevertheless, the underestimation of the NO_3^- concentration due to underestimating the liquid-water content might be balanced out or even overwhelmed if the deposition of other acidic solutes increase, such as HCl or H_2SO_4, on the surface snow, which lower the pH and reduce the solubility of HNO_3 in the micropocket. Note that the micropockets only existed at temperature higher than the eutectic temperature, for simplification, the eutectic temperature was assumed to be the eutectic temperature of the system of H_2O and the most abundant solute within surface snow. However, in reality, the presence of other impurities might have an impact on that and would require confirmation with future experimental data.

7 Conclusions

Two physical models were developed from first principles to estimate the bulk NO_3^- concentration in the skin layer of snow using observed atmospheric nitrate concentration, temperature and humidity as inputs. Model 1, based on the assumption of a homogeneous DI as the interface between air and snow grain above 238 K and Model 2, based on the hypothesis of majority of snow crystal surfaces being ice and liquid is located in grooves at grain boundaries and triple junction above the eutectic temperature.

The modelled skin layer NO_3^- concentration from Model 1 are reasonably well agreed with observations from the cold Dome C but overestimated by an order of magnitude at the relatively warmer Halley. The uncertainties in Model 1 are the temperature threshold, T_o, that define the 'Air-DI' interface and the partition coefficient of DI. The poor performance of Model 1 at the warmer site supports the argument in previous studies (Bartels-Rausch et al., 2014; Domine et al., 2013) that the disordered interface cannot be parameterised as a thin, homogenous water-like layer coving the entire grain surface and its interactions with the solutes are not the same as in aqueous phase.

Model 2 reproduced the skin layer NO_3^- concentration with good agreement at both Dome C and Halley without any tuning parameters. This indicated the major interface between skin layer snow grain and surrounding air can well be 'Air-Ice' with liquid formed by impurities presented as micropocket as suggested by Domine et al. (2013). The interaction of nitrate between the air and skin layer snow can be described as a combination of non-equilibrium kinetic ice surface adsorption and co-condensation coupled with solid diffusion within grain in the winter. During summer, the equilibrium solvation in liquid micropocket dominate the exchange of nitrate between air and skin layer snow. Additional modelling studies, e.g. including uptake of other chemical species or aerosols, backed up by field observations from other locations with various meteorological conditions as well

Atmos. Chem. Phys. Discuss., doi:10.5194/acp-2016-1069, 2016
Manuscript under review for journal Atmos. Chem. Phys.
Published: 15 December 2016

Atmospheric Chemistry and Physics Discussions

as laboratory studies on eutectic point of a multi-ions - H_2O system, uptake coefficient at higher temperature, are needed to confirm the representativeness and improve performance of Model 2.

Despite the simplified parameterisation of processes in Model 2, such as the impurities content in snow, liquid pockets located in different locations were treated as one and had the same chemical properties as bulk liquid, it is still sufficient enough to be implemented in regional and global atmospheric chemistry models and possibly improve the accuracy of the boundary layer chemistry and oxidation capacity. As mentioned in the Sect. 3 both models developed here are purely physical as the uptake processes overwhelm the photochemical processes in the skin layer snow, however, this assumption is not be applicable to the entire snowpack (Frey et al., 2009; France et al., 2011; Erbland et al., 2013). Other processes, such as chemical and photochemical processes needs to be included within the model to be implemented into a 1-D Air-Snow model to estimate the vertical profile of NO_3^- concentration.

Acknowledgements. HGC is funded by the Natural Environment Research Council through Doctoral Studentship NE/L501633/1. We are thankful to our colleagues (Anna Jones, Neil Brough and Xin Yang) for helpful discussion.

Atmos. Chem. Phys. Discuss., doi:10.5194/acp-2016-1069, 2016
Manuscript under review for journal Atmos. Chem. Phys.
Published: 15 December 2016

Atmospheric Chemistry and Physics Discussions

8 Notation

Table 1. Notation of constants and parameters

Symbol	Description	units
α	Accommodation coefficient	dimensionless
$\mathrm{A_{ice}}$	Surface area of ice per unit volume of snowpack	$\mathrm{m^2\,m^{-3}_{snowpack}}$
$\mathrm{C_v(RMSE)}$	Coefficient of variation	N/A
DI	Disordered Interface	N/A
D_v	Water vapour diffusivity	$\mathrm{m^2\,s^{-1}}$
$[\mathrm{HNO_{3\,(ads)}}]$	Nitric acid concentration contributed by surface adsorption	$\mathrm{molecule\,m^{-3}}$
$[\mathrm{HNO_{3\,(cc)}}]$	Nitric acid concentration contributed by co-condensation	$\mathrm{molecule\,m^{-3}}$
$[\mathrm{HNO_{3\,(DI)}}]$	Nitric acid concentration in the DI	$\mathrm{molecule\,m^{-3}}$
$[\mathrm{HNO_{3\,(ice)}}]$	Nitric acid concentration in solid ice	$\mathrm{molecule\,m^{-3}}$
$[\mathrm{HNO_{3\,(surf)}}]$	Nitric acid concentration on surface of grain	$\mathrm{molecule\,m^{-3}}$
k_{ads}	Adsorption coefficient on ice	$\mathrm{m^3\,molecule^{-1}\,s^{-1}}$
k_{des}	Desorption coefficient on ice	$\mathrm{s^{-1}}$
$k_{\mathrm{H^{cc}}}$	Henry's Law coefficient	dimensionless
$k_{\mathrm{H}}^{\mathrm{eff}}$	Effective Henry's Law coefficient	dimensionless
k_{diff}	Diffusion coefficient in ice	$\mathrm{m^2\,s^{-1}}$
$\mathrm{K_a}$	Acid dissociation constant	$\mathrm{molecule\,m^{-3}}$
$\mathrm{K_{eq}}$	Equilibrium constant for Langmuir adsorption	$\mathrm{m^3\,molecule^{-1}}$
N_{max}	Maximum number of adsorption sites	$\mathrm{molecule\,m^{-2}}$
$[\mathrm{NO^-_{3\,(bulk)}}]$	Bulk nitrate concentration	$\mathrm{molecule\,m^{-3}}$
$\phi_{\mathrm{H_2O}}$	Liquid water fraction	dimensionless
$\Phi^{\mathrm{aq}}_{\mathrm{bulk}}$	Fraction of the total amount of solute in aqueous phase	dimensionless
R_{eff}	Effective radius of snow grain derived from SSA data	m
ρ_{ice}	Density of ice	$\mathrm{kg\,m^{-3}}$
ρ_v	Water vapour density	$\mathrm{kg\,m^{-3}}$
[S]	Number of available surface sites per unit volume of air	$\mathrm{molecule\,m^{-3}_{air}}$
SSA	Specific surface area	$\mathrm{m^2\,kg^{-1}}$
T_e	Eutectic temperature	K
T_f	Reference temperature	K
T_o	Threshold temperature in Model 1	K
$\overline{v}$	Mean molecular speed	$\mathrm{m\,s^{-1}}$
V_{air}	Volume of air per unit volume of snowpack	$\mathrm{m^3_{air}\,m^{-3}_{snowpack}}$
V_{grain}	Volume of a snow grain	$\mathrm{m^3}$

Atmos. Chem. Phys. Discuss., doi:10.5194/acp-2016-1069, 2016
Manuscript under review for journal Atmos. Chem. Phys.
Published: 15 December 2016

Atmospheric Chemistry and Physics Discussions

Table 2. Summary of model performance at Dome C based on the coefficient of variation of RMSE, $C_v(\mathrm{RMSE})$

Model description	Short name	Whole year DOY 30 - 385	Winter-Spring DOY 90 - 318	Summer DOY 319 - 385
Surface Adsorption & Solid Diffusion	Kinetic Approach	-	0.65	-
Ice Solubility & Solid Diffusion	Equilibrium Approach	-	0.52	-
Surface Adsorption-Co Condensation/DI Solvation & Solid Diffusion				
No threshold (no Solvation)	Model 1-none	1.07	0.65	0.88
Threshold $\leq$ 238 K	Model 1-238K	1.34	0.73	1.11
Threshold $\leq$ 240 K	Model 1-240K	0.50	0.64	0.36
Threshold $\leq$ 242 K	Model 1-242K	0.61	0.65	0.46
Surface Adsorption-Co Condensation & Solid Diffusion + micropocket	Model 2	0.84		0.67

Table 3. Summary of model performance at Halley based on the coefficient of variation of RMSE, $C_v(\mathrm{RMSE})$

Model description	Short name	Whole year DOY 87 - 406	Winter DOY 90 - 257	Spring -Early Autumn DOY 258 - 406
Surface Adsorption & Solid Diffusion	Kinetic Approach	-	1.13	-
Ice Solubility & Solid Diffusion	Equilibrium Approach	-	1.12	-
Surface Adsorption-Co Condensation/DI Solvation & Solid Diffusion				
No threshold (no Solvation)	Model 1-none	1.06	1.06	0.95
Threshold $\leq$ 238 K	Model 1-238K	89.28	27.78	87.15
Threshold $\leq$ 242 K	Model 1-242K	50.76	23.86	49.00
Surface Adsorption-Co Condensation & Solid Diffusion + micropocket	Model 2	0.84	1.08	0.65

Atmos. Chem. Phys. Discuss., doi:10.5194/acp-2016-1069, 2016
Manuscript under review for journal Atmos. Chem. Phys.
Published: 15 December 2016

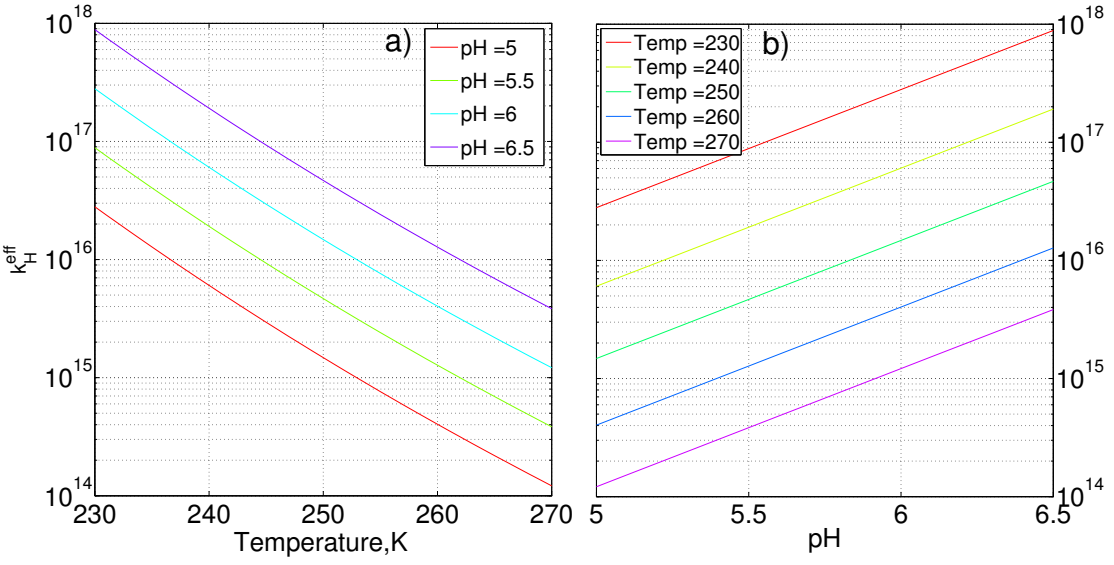

Figure 1. The dependence of the effective Henry's Law coefficient, $k_{\mathrm{H^{eff}}}$, of HNO_3 on temperature (a.) and pH (b.)

Atmos. Chem. Phys. Discuss., doi:10.5194/acp-2016-1069, 2016
Manuscript under review for journal Atmos. Chem. Phys.
Published: 15 December 2016

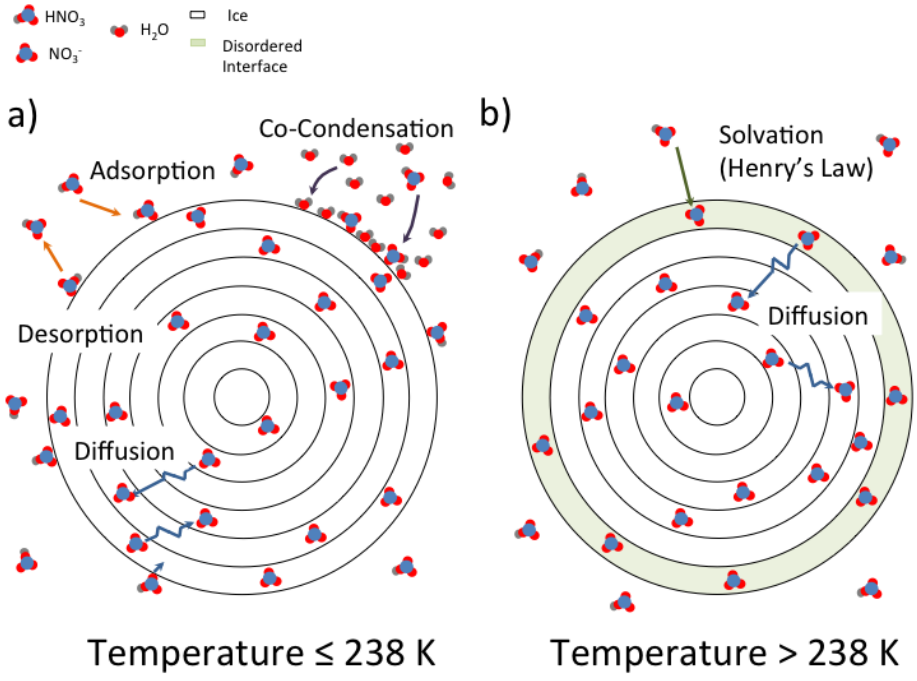

Figure 2. Schematic of Model 1. a) At temperatures below 238 K the concentration of NO_3^- at the surface of the snow grain is determined by Air-Ice processes, i.e. non-equilibrium adsorption and co-condensation. b) At temperatures above 238 K the concentration of NO_3^- at the surface of the snow grain is determined by Air-DI processes, i.e. non-equilibrium solvation.

Atmos. Chem. Phys. Discuss., doi:10.5194/acp-2016-1069, 2016
Manuscript under review for journal Atmos. Chem. Phys.
Published: 15 December 2016

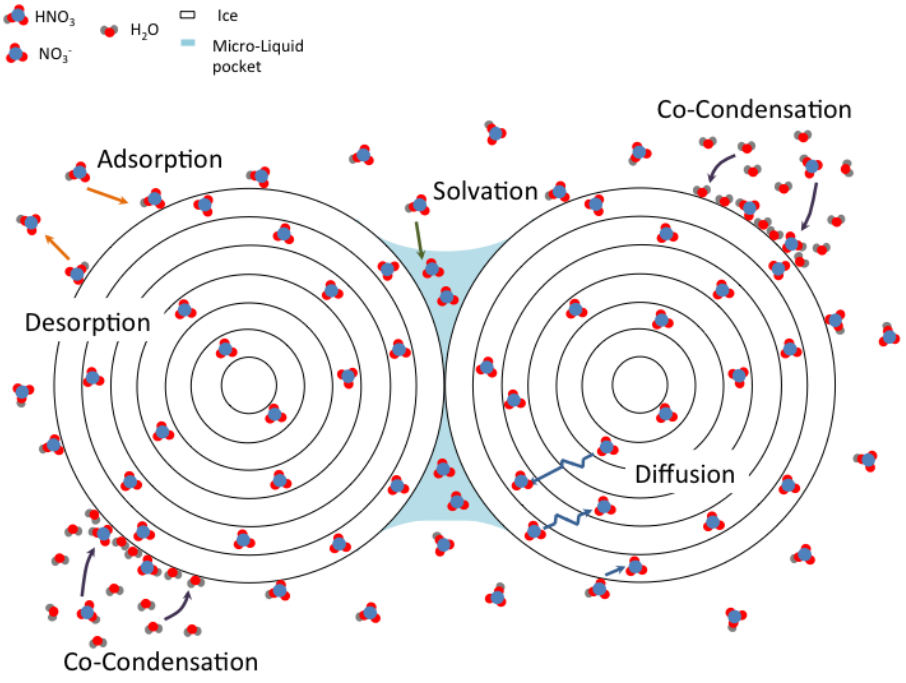

Figure 3. Schematic of Model 2. At all temperatures below melting, the concentration of NO_3^- at the surface of the snow grain is determined by Air-Ice processes, i.e. non-equilibrium adsorption and co-condensation. At temperatures above the eutectic temperature, liquid is assumed to co-exist with ice and the liquid fraction is in the form of micropockets that are located at grain boundaries and triple junctions (Domine et al., 2013).

Atmos. Chem. Phys. Discuss., doi:10.5194/acp-2016-1069, 2016
Manuscript under review for journal Atmos. Chem. Phys.
Published: 15 December 2016

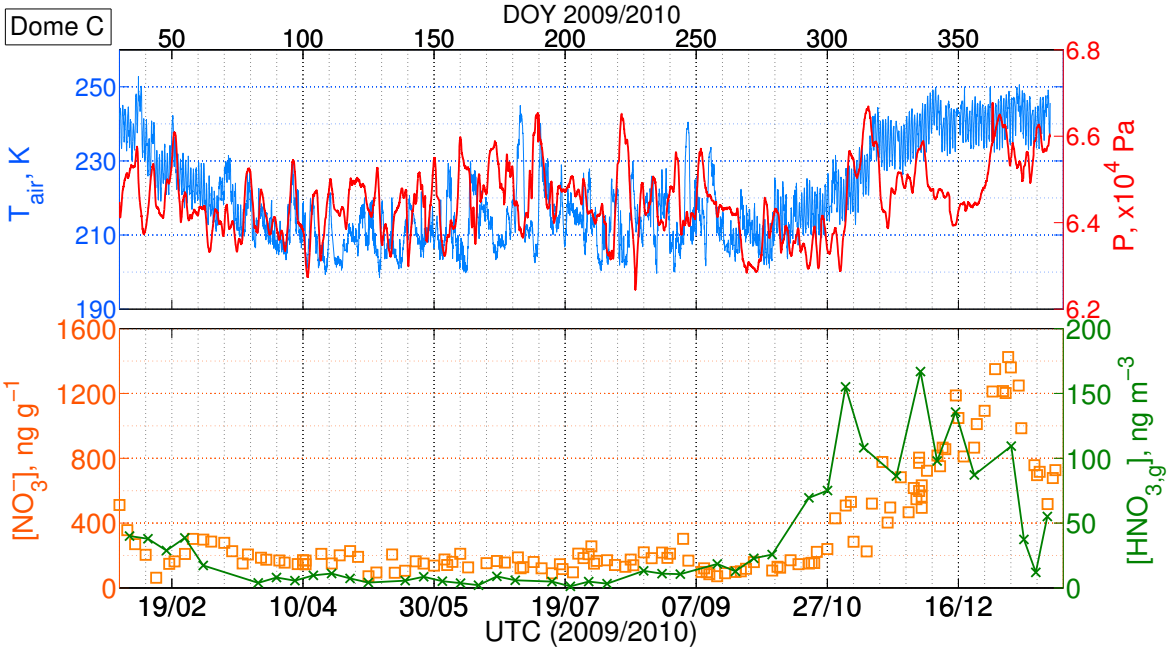

Figure 4. Atmospheric and snow observations from Dome C (Erbland et al., 2013). Top: Air temperature (blue, left axis) and atmospheric pressure (red, right axis). Bottom: skin layer snow (i.e. top 4 ± 2 mm) nitrate concentrations (orange square, left axis) and atmospheric nitrate concentrations, sum of the atmospheric particulate nitrate and HNO_3 (green, right axis).

Atmos. Chem. Phys. Discuss., doi:10.5194/acp-2016-1069, 2016
Manuscript under review for journal Atmos. Chem. Phys.
Published: 15 December 2016

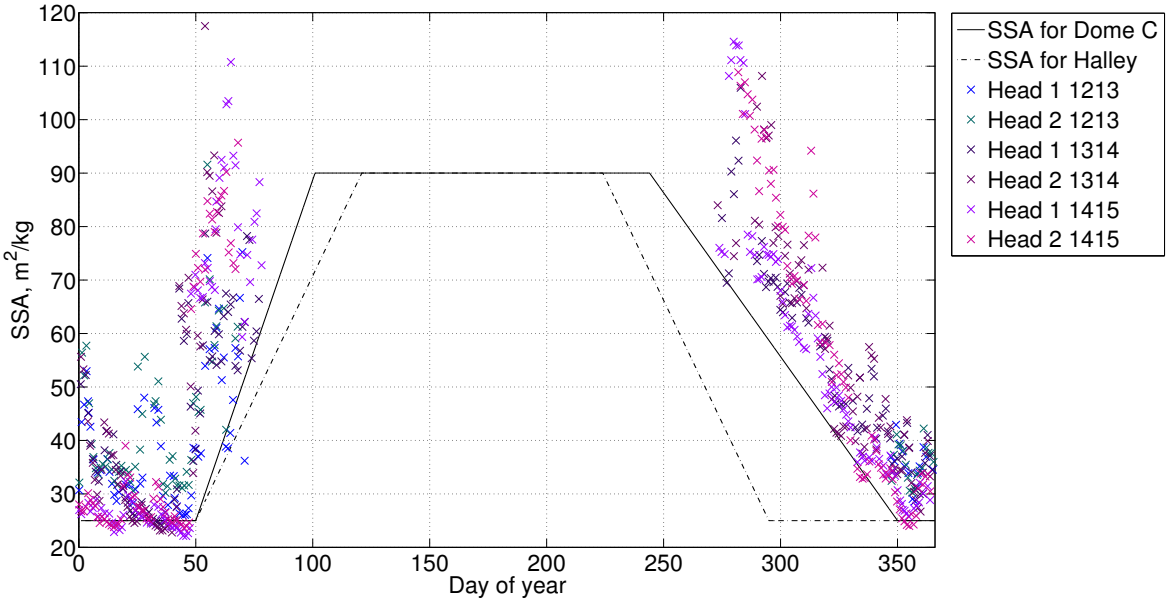

Figure 5. Year-round estimates of SSA fro Dome C (−) and Halley (−·) are based on observations at Dome C from 2012 to 2015 by Picard et al. (2016). The SSA estimates for Halley take into account the shorter cold period compare to Dome C, which tends to have larger SSA.

Atmos. Chem. Phys. Discuss., doi:10.5194/acp-2016-1069, 2016
Manuscript under review for journal Atmos. Chem. Phys.
Published: 15 December 2016

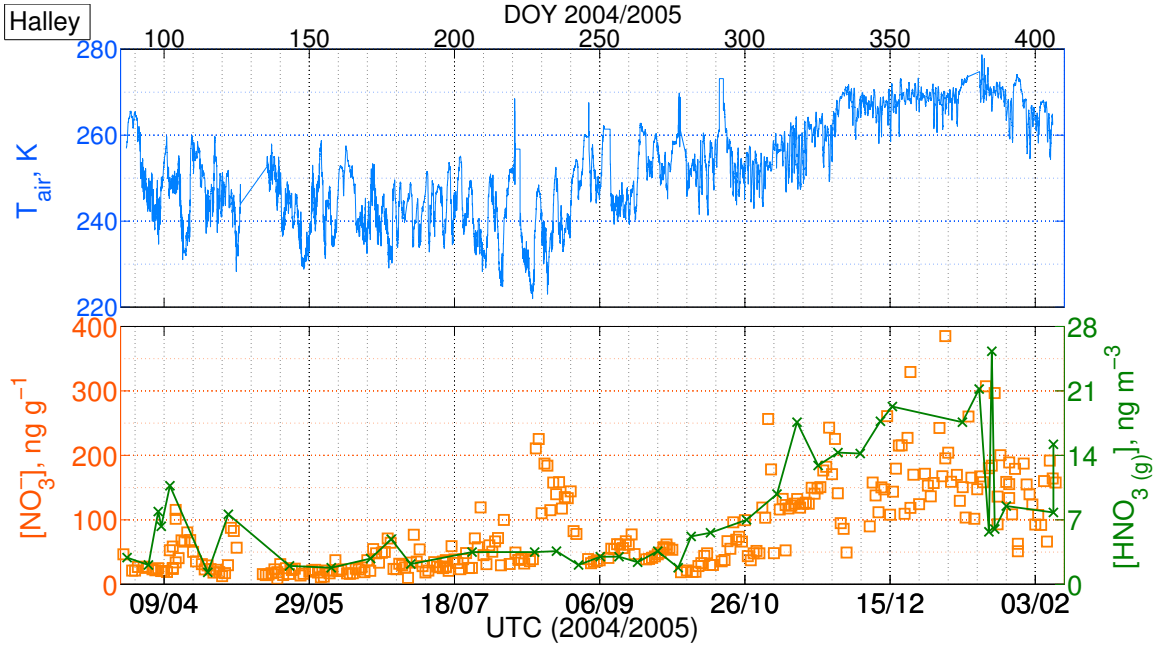

Figure 6. Atmospheric and snow observations at Halley between 27$^{\text{th}}$ March 2004 and 9$^{\text{th}}$ February 2005 (Jones et al., 2008). Top: Air temperature. Bottom: surface snow, the top 10 ± 15 mm, nitrate concentrations (orange square, left axis) and gas-phase nitric acid concentrations (green, right axis).

Atmos. Chem. Phys. Discuss., doi:10.5194/acp-2016-1069, 2016
Manuscript under review for journal Atmos. Chem. Phys.
Published: 15 December 2016

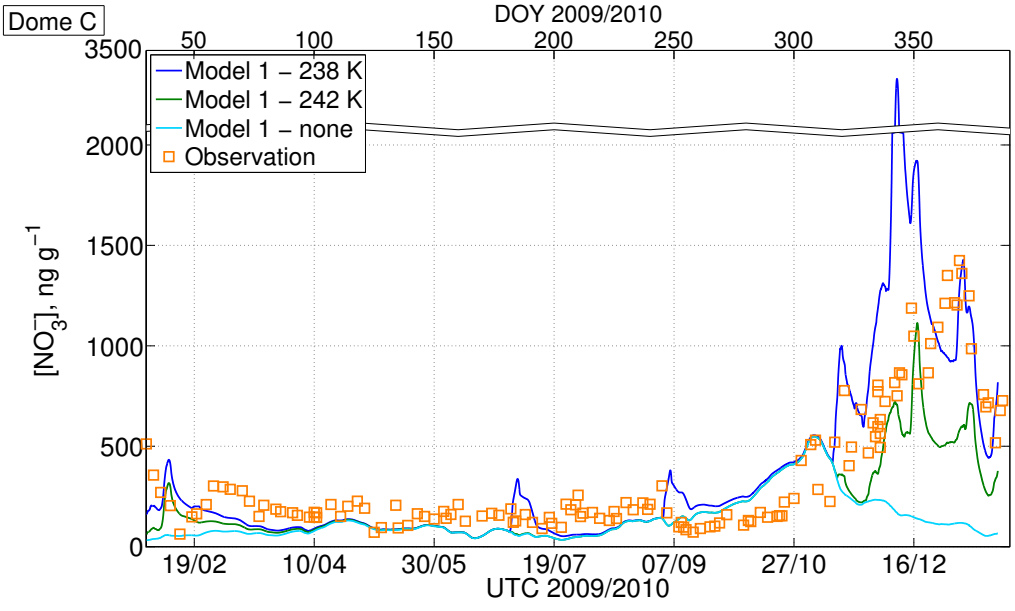

Figure 7. Model 1 output of Dome C skin layer snow NO_3^- concentration. At temperatures less than the threshold temperature, T_o, the interface between air and snow grain is assumed to be ice ('Air-Ice') and the NO_3^- concentration is determined by a combination of non-equilibrium adsorption on ice and co-condensation coupled with solid-state diffusion. Above T_o, the interface between air and snow grain is assumed to be DI ('Air-DI'), i.e. the NO_3^- concentration is determined by combination of non-equilibrium solvation in DI coupled with solid-state diffusion. Dark blue: T_o set as 238 K; Green: T_o set as 242 K; Light blue: 'Air-Ice', i.e. T_o set as the melting temperature; Orange squares: observation.

Atmos. Chem. Phys. Discuss., doi:10.5194/acp-2016-1069, 2016
Manuscript under review for journal Atmos. Chem. Phys.
Published: 15 December 2016

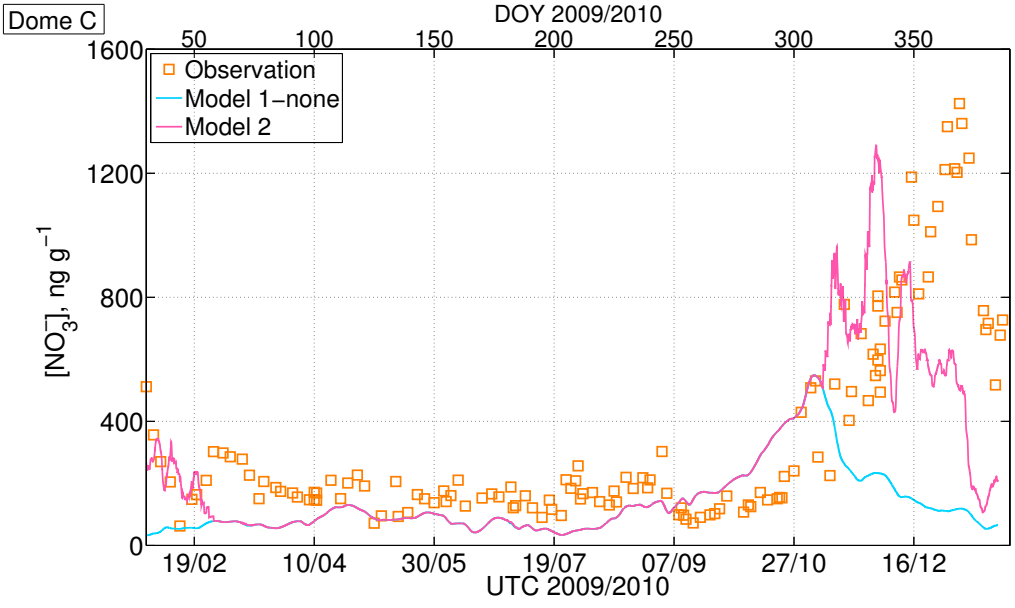

Figure 8. Model 2 output of Dome C skin layer snow NO_3^- concentration. The major interface between air and snow is assumed to be ice ('Air-Ice') at all temperatures below melting and the NO_3^- concentration in ice is determined by a combination of non-equilibrium adsorption and co-condensation coupled with solid-state diffusion. Above eutectic temperature, T_e (230 K), liquid co-existed with ice in the form of micropocket. The partition between air and micropocket is determined by Henry's law. Pink: 'Air-Ice' plus micropocket; Light Blue: 'Air-Ice'; Orange squares: observation.

Atmos. Chem. Phys. Discuss., doi:10.5194/acp-2016-1069, 2016
Manuscript under review for journal Atmos. Chem. Phys.
Published: 15 December 2016

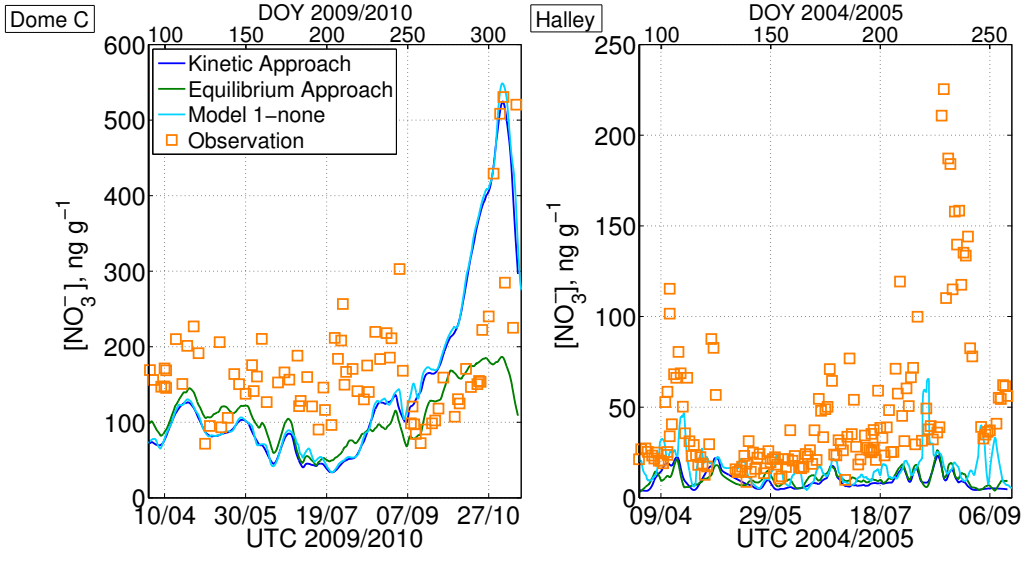

Figure 9. Comparison of the nitrate Air-Ice interaction between the 'Equilibrium' approach (similar to Bock et al. (2016), in green), the 'Kinetic' approach (this work, in dark blue) and the contribution from co-condensation process (this work: Model 1- none, in light blue) in winter. The 'Kinetic' approach describes the interaction as non-equilibrium kinetic surface adsorption coupled with solid diffusion inside the grain whereas the 'Equilibrium' approach describes the interaction as equilibrium solubility coupled with solid diffusion inside the grain.

Atmos. Chem. Phys. Discuss., doi:10.5194/acp-2016-1069, 2016
Manuscript under review for journal Atmos. Chem. Phys.
Published: 15 December 2016

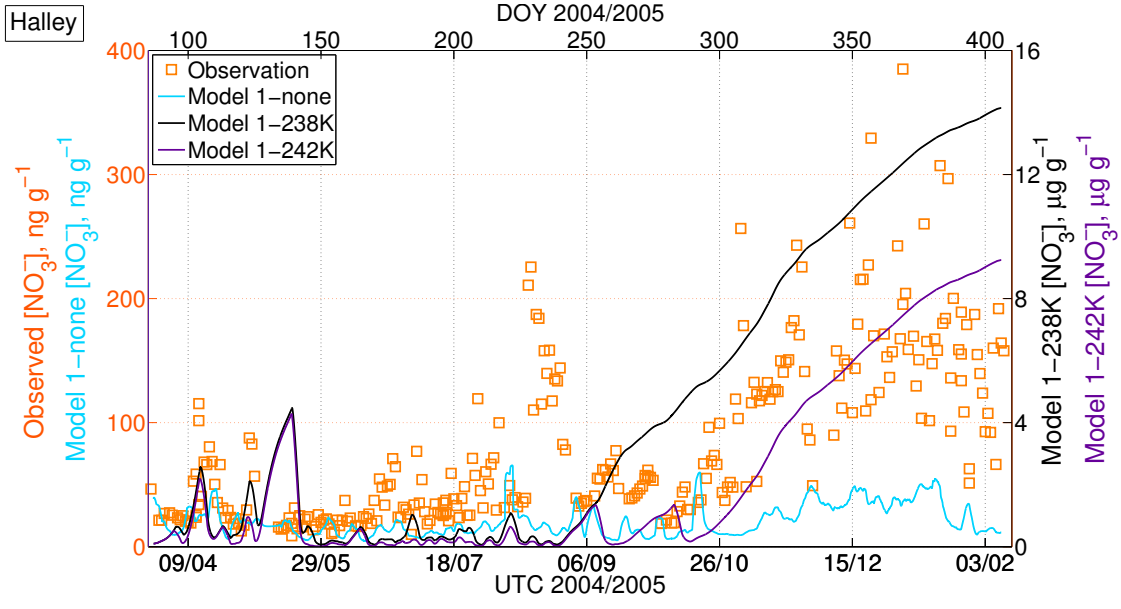

Figure 10. Model 1 output of Halley skin layer snow NO_3^- concentration. At temperatures less than the threshold temperature, T_o, the interface between air and snow grain is assumed to be ice ('Air-Ice') and the NO_3^- concentration is determined by a combination of non-equilibrium adsorption on ice and co-condensation coupled with solid-state diffusion. At temperature above T_o, the interface between air and snow grain is assumed to be DI ('Air-Ice'), that the NO_3^- concentration is determined by combination of non-equilibrium solvation in DI coupled with solid-state diffusion. Black (Right axis): T_o set as 238 K; Purple (Right axis): T_o set as 242 K; Light blue (Left axis) : 'Air-Ice', i.e. T_o set as the melting temperature; Orange square (Left axis) - observation.

Atmos. Chem. Phys. Discuss., doi:10.5194/acp-2016-1069, 2016
Manuscript under review for journal Atmos. Chem. Phys.
Published: 15 December 2016

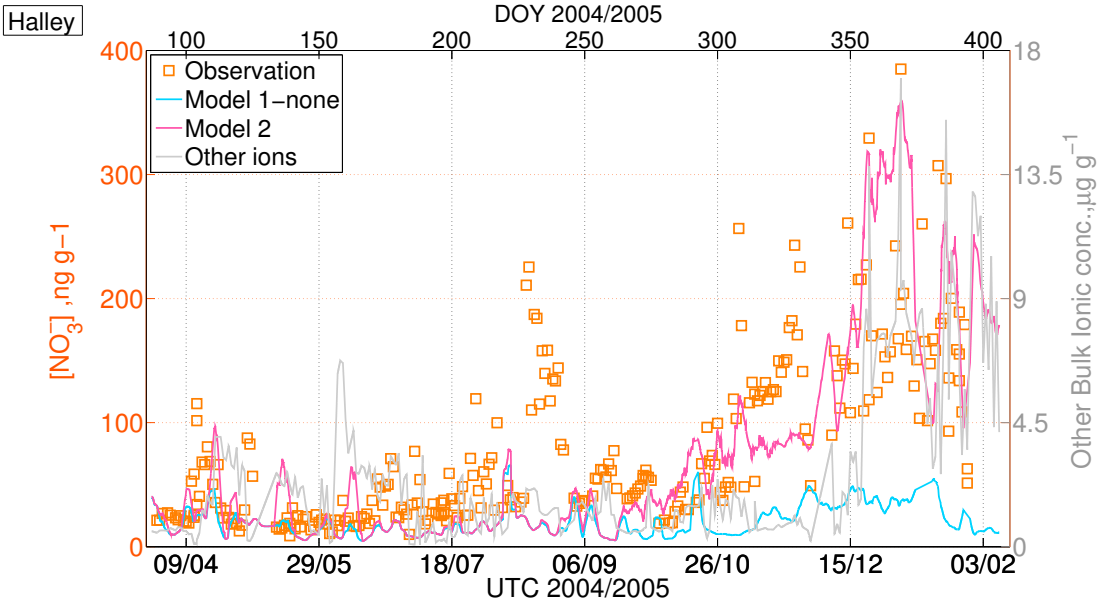

Figure 11. Model 2 output of Halley skin layer snow NO_3^- concentration. The major interface between air and snow is assumed to be ice ('Air-Ice') at all temperature below melting and the NO_3^- concentration in ice is determined by a combination of non-equilibrium adsorption and co-condensation coupled with solid-state diffusion. Above eutectic temperature, T_e (252 K), liquid co-existes with ice in the form of micropocket. The partition between air and micropocket is determined by Henry's law. Pink: 'Air-Ice' plus micropocket interaction ; Light Blue: 'Air-Ice' only interaction; Orange squares: observation. Grey (Right axis) - measured bulk concentration of other ions, e.g. $[Na^+]$ + $[Cl^-]$.

Atmos. Chem. Phys. Discuss., doi:10.5194/acp-2016-1069, 2016
Manuscript under review for journal Atmos. Chem. Phys.
Published: 15 December 2016

Atmospheric Chemistry and Physics Discussions

Appendix A: Air-Ice interface

Table A1. Parameterisation for HNO_3

Symbol	Parameter	Value/Parameterisation	units	Reference
α_0	Accommodation coefficient at standard temperature	3×10^{-3} [i]	Dimensionless	Hudson et al. (2002)
k_{diff}	Diffusion coefficient of nitrate in ice	$1.37 \times 10^{-2610/T}$	$\mathrm{cm^2\,s^{-1}}$	Thibert et al. (1998)
$\Delta_{\mathrm{sol}}H$	Enthalpy of solution at standard temperature	72.3	$\mathrm{kJ\,mol^{-1}}$	Brimblecombe and Clegg (1988)
$\Delta_{\mathrm{obs}}H$	Enthalpy of activation	44	$\mathrm{kJ\,mol^{-1}}$	Sander (2015)
k^0_{H}	Henry constant at 298 K	1.7×10^5 [ii]	$\mathrm{M\,atm^{-1}}$	Brimblecombe and Clegg (1988)
N_{max}	Maximum adsorption site	2.7×10^{18}	$\mathrm{molecules\,m^{-2}}$	Crowley et al. (2010)
$\overline{v}$	Mean molecular speed	$\sqrt{\frac{8RT}{M_m \pi}}$ [iii]	$\mathrm{m\,s^{-1}}$	Sander (1999)
$X^0_{\mathrm{HNO_3}}$	Molar fraction of HNO_3 in ice	$X^0_{\mathrm{HNO_3}} = 2.37 \times 10^{-12} \exp(\frac{3532.2}{T}) P^{1/2.3}_{\mathrm{HNO_3}}$	$\mathrm{mol\,mol^{-1}}$	Thibert et al. (1998)
K_{eq}	Langmuir adsorption equilibrium constant	$-8.2 \times 10^{-18}\mathrm{T} + 2.01 \times 10^{-15}$	$\mathrm{m^3 molecule^{-1}}$	Burkholder and Wine (2015)
D_v	Water vapour diffusivity	$D_v = 2.11 \times 10^{-5} (\frac{T}{T_c})^{1.94} \frac{P_c}{P}$	$\mathrm{m^2\,s^{-1}}$	Pruppacher and Klett (1997)

[i] Temperature dependent accommodation coefficient, $\alpha = \frac{\exp\{\ln(\frac{\alpha_0}{1-\alpha_0}) - \frac{\Delta_{\mathrm{obs}}H}{R}(\frac{1}{T} - \frac{1}{T_f})\}}{1-\exp\{\ln(\frac{\alpha_0}{1-\alpha_0}) - \frac{\Delta_{\mathrm{obs}}H}{R}(\frac{1}{T} - \frac{1}{T_f})\}}$, where R is the molar gas constant, T is the temperature, $\mathrm{T_f}$ is the reference temperature (220 K)

[ii] Temperature dependent dimensionless Henry's Law coefficient, $k^{cc}_{\mathrm{H}} = k^0_{\mathrm{H}} \times RT \times \exp\left(\frac{-\Delta_{\mathrm{sol}}H}{R}\left(\frac{1}{T} - \frac{1}{T^{\ominus}}\right)\right)$, where $T^{\ominus}$ is the standard temperature (258 K).

[iii] M_m is the molar mass of the gas.

Atmos. Chem. Phys. Discuss., doi:10.5194/acp-2016-1069, 2016
Manuscript under review for journal Atmos. Chem. Phys.
Published: 15 December 2016

Atmospheric Chemistry and Physics Discussions

References

Akinfiev, N. N., Mironenko, M. V., and Grant, S. A.: Thermodynamic Properties of NaCl Solutions at Subzero Temperatures, Journal of Solution Chemistry, 30, 1065–1080, doi:10.1023/A:1014445917207, http://dx.doi.org/10.1023/A:1014445917207, 2001.

Argentini, S., Pietroni, I., Mastrantonio, G., Viola, A. P., Dargaud, G., and Petenko, I.: Observations of near surface wind speed, temperature and radiative budget at Dome C, Antarctic Plateau during 2005, Antarctic Science, 26, 104–112, doi:10.1017/S0954102013000382, 2014.

Arthern, R. J., Winebrenner, D. P., and Vaughan, D. G.: Antarctic snow accumulation mapped using polarization of 4.3-cm wavelength microwave emission, Journal of Geophysical Research: Atmospheres, 111, n/a–n/a, doi:10.1029/2004JD005667, http://dx.doi.org/10.1029/2004JD005667, d06107, 2006.

Bartels-Rausch, T., Jacobi, H.-W., Kahan, T. F., Thomas, J. L., Thomson, E. S., Abbatt, J. P. D., Ammann, M., Blackford, J. R., Bluhm, H., Boxe, C., Domine, F., Frey, M. M., Gladich, I., Guzmán, M. I., Heger, D., Huthwelker, T., Klán, P., Kuhs, W. F., Kuo, M. H., Maus, S., Moussa, S. G., McNeill, V. F., Newberg, J. T., Pettersson, J. B. C., Roeselová, M., and Sodeau, J. R.: A review of air, ice chemical and physical interactions (AICI): liquids, quasi-liquids, and solids in snow, Atmospheric Chemistry and Physics, 14, 1587–1633, doi:10.5194/acp-14-1587-2014, http://www.atmos-chem-phys.net/14/1587/2014/, 2014.

Beine, H. J., Honrath, R. E., DominÈ, F., Simpson, W. R., and Fuentes, J. D.: NOx during background and ozone depletion periods at Alert: Fluxes above the snow surface, Journal of Geophysical Research: Atmospheres, 107, ACH 7–1–ACH 7–12, doi:10.1029/2002JD002082, http://dx.doi.org/10.1029/2002JD002082, 4584, 2002.

Beyer, K. D., , and Hansen, A. R.: Phase Diagram of the Nitric Acid/Water System: Implications for Polar Stratospheric Clouds, The Journal of Physical Chemistry A, 106, 10 275–10 284, doi:10.1021/jp025535o, http://dx.doi.org/10.1021/jp025535o, 2002.

Bock, J., Savarino, J., and Picard, G.: Air–snow exchange of nitrate: a modelling approach to investigate physicochemical processes in surface snow at Dome C, Antarctica, Atmospheric Chemistry and Physics, 16, 12 531–12 550, doi:10.5194/acp-16-12531-2016, http://www.atmos-chem-phys.net/16/12531/2016/, 2016.

Boxe, C. S. and Saiz-Lopez, A.: Multiphase modeling of nitrate photochemistry in the quasi-liquid layer (QLL): implications for NO_x release from the Arctic and coastal Antarctic snowpack, Atmospheric Chemistry and Physics, 8, 4855–4864, doi:10.5194/acp-8-4855-2008, http://www.atmos-chem-phys.net/8/4855/2008/, 2008.

Brimblecombe, P. and Clegg, S. L.: The solubility and behaviour of acid gases in the marine aerosol, Journal of Atmospheric Chemistry, 7, 1–18, doi:10.1007/BF00048251, http://dx.doi.org/10.1007/BF00048251, 1988.

Burkholder,J. B. , Sander, S. P. , Abbatt, J. P., Barker, J. R., Huie, R. E., Kolb, C. E., Kurylo, M. J., Orkin, V. L., Wilmouth, D. M., Wine, P. H. : Chemical Kinetics and Photochemical Data for Use in Atmospheric Studies, Evaluation No. 18, JPL Publication 15-10, Jet Propulsion Laboratory, Pasadena, 2015.

Cho, H., Shepson, P. B., Barrie, L. A., Cowin, J. P., Zaveri, R.: NMR Investigation of the QuasiBrine Layer in Ice/Brine Mixtures, The Journal of Physical Chemistry B, 106, 11 226–11 232, doi:10.1021/jp020449, http://dx.doi.org/10.1021/jp020449+, 2002.

Conde, M. M., Vega, C., and Patrykiejew, A.: The thickness of a liquid layer on the free surface of ice as obtained from computer simulation, The Journal of Chemical Physics, 129,

014702, doi:http://dx.doi.org/10.1063/1.2940195, http://scitation.aip.org/content/aip/journal/jcp/129/1/10.1063/1.2940195, 2008.

Cox, R. A., Fernandez, M. A., Symington, A., Ullerstam, M., and Abbatt, J. P. D.: A kinetic model for uptake of HNO3 and HCl on ice in a coated wall flow system, Phys. Chem. Chem. Phys., 7, 3434–3442, doi:10.1039/B506683B, http://dx.doi.org/10.1039/B506683B, 2005.

Crowley, J. N., Ammann, M., Cox, R. A., Hynes, R. G., Jenkin, M. E., Mellouki, A., Rossi, M. J., Troe, J., and Wallington, T. J.: Evaluated kinetic and photochemical data for atmospheric chemistry: Volume V ,§? heterogeneous reactions on solid substrates, Atmospheric Chemistry and Physics, 10, 9059–9223, doi:10.5194/acp-10-9059-2010, http://www.atmos-chem-phys.net/10/9059/2010/, 2010.

Domine, F., Bock, J., Voisin, D., and Donaldson, D. J.: Can We Model Snow Photochemistry? Problems with the Current Approaches, The Journal of Physical Chemistry A, 117, 4733–4749, doi:10.1021/jp3123314, http://dx.doi.org/10.1021/jp3123314, pMID: 23597185, 2013.

Erbland, J., Vicars, W. C., Savarino, J.,Morin, S., Frey, M. M., Frosini, D., Vince, E., Martins, J. M. F.: Air snow transfer of nitrate on the East Antarctic Plateau Part 1: Isotopic evidence for a photolytically driven dynamic equilibrium in summer , Atmospheric Chemistry and Physics, 13, 6403–6419, doi:10.5194/acp-13-6403-2013, http://www.atmos-chem-phys.net/13/6403/2013/, 2013.

Fowler, D., Amann, M., Anderson, F., Ashmore, M., Cox, P., Depledge, M., Derwent, D., Grennfelt, P., Hewitt, N., Hov, O., Jenkin, M., Kelly, F., Liss, P. S., Pilling, M., Pyle, J., Slingo, J. and Stevenson, D.: Ground-level ozone in the 21st century: future trends, impacts and policy implications, vol. 15/08 of *Science Policy*, The Royal Society, London, http://nora.nerc.ac.uk/8577/, prof. David Fowler was Chair of the Working Group, 2008.

France, J. L., King, M. D., Frey, M. M., Erbland, J., Picard, G., Preunkert, S., MacArthur, A., and Savarino, J.: Snow optical properties at Dome C (Concordia), Antarctica; implications for snow emissions and snow chemistry of reactive nitrogen, Atmospheric Chemistry and Physics, 11, 9787–9801, doi:10.5194/acp-11-9787-2011, http://www.atmos-chem-phys.net/11/9787/2011/, 2011.

Frey, M. M., Savarino, J., Morin, S., Erbland, J., and Martins, J. M. F.: Photolysis imprint in the nitrate stable isotope signal in snow and atmosphere of East Antarctica and implications for reactive nitrogen cycling, Atmospheric Chemistry and Physics, 9, 8681–8696, doi:10.5194/acp-9-8681-2009, http://www.atmos-chem-phys.net/9/8681/2009/, 2009.

Flanner, M. G. and Zender, C. S.: Linking snowpack microphysics and albedo evolution, Journal of Geophysical Research: Atmospheres, 111, n/a–n/a, doi:10.1029/2005JD006834, http://dx.doi.org/10.1029/2005JD006834, d12208, 2006.

Gligorovski, S., Strekowski, R., Barbati, S., and Vione, D.: Environmental Implications of Hydroxyl Radicals (OH), Chemical Reviews, 115, 13 051–13 092, doi:10.1021/cr500310b, http://dx.doi.org/10.1021/cr500310b, pMID: 26630000, 2015.

Grannas, A. M., Jones, A. E., Dibb, J., Ammann, M., Anastasio, C., Beine, H. J., Bergin, M., Bottenheim, J., Boxe, C. S., Carver, G., Chen, G., Crawford, J. H., Dominé, F., Frey, M. M., Guzmán, M. I., Heard, D. E., Helmig, D., Hoffmann, M. R., Honrath, R. E., Huey, L. G., Hutterli, M., Jacobi, H. W., Klán, P., Lefer, B., McConnell, J., Plane, J., Sander, R., Savarino, J., Shepson, P. B., Simpson, W. R., Sodeau, J. R., von Glasow, R., Weller, R., Wolff, E. W., and Zhu, T.: An overview of snow photochemistry: evidence, mechanisms

and impacts, Atmospheric Chemistry and Physics, 7, 4329–4373, doi:10.5194/acp-7-4329-2007, http://www.atmos-chem-phys.net/7/4329/2007/, 2007.

Honrath, R. E., Peterson, M. C., Dziobak, M. P., Dibb, J. E., Arsenault, M. A., and Green, S. A.: Release of NOx from sunlight-irradiated midlatitude snow, Geophysical Research Letters, 27, 2237–2240, doi:10.1029/1999GL011286, http://dx.doi.org/10.1029/1999GL011286, 2000.

Hudson, P. K., Zondlo, M. A., , and Tolbert*, M. A.: The Interaction of Methanol, Acetone, and Acetaldehyde with Ice and Nitric Acid-Doped Ice: Implications for Cirrus Clouds, The Journal of Physical Chemistry A, 106, 2882–2888, doi:10.1021/jp012718m, http://dx.doi.org/10.1021/jp012718m, 2002.

Hutterli, M. A. and Röthlisberger, R.: Atmosphere-to-snow-to-firn transfer studies of HCHO at Summit, Greenland, GEOPHYSICAL RESEARCH LETTERS, 26, 1691–1694, 1999.

Hutterli, M. A., McConnell, J. R., Bales, R. C., and Stewart, R. W.: Sensitivity of hydrogen peroxide (H2O2) and formaldehyde (HCHO) preservation in snow to changing environmental conditions: Implications for ice core records, Journal of Geophysical Research: Atmospheres, 108, ACH 6–1–ACH 6–9, doi:10.1029/2002JD002528, http://dx.doi.org/10.1029/2002JD002528, 4023, 2003.

Jones, A. E., Weller, R., Anderson, P. S., Jacobi, H.-W., Wolff, E. W., Schrems, O., and Miller, H.: Measurements of NOx emissions from the Antarctic snowpack, Geophysical Research Letters, 28, 1499–1502, doi:10.1029/2000GL011956, http://dx.doi.org/10.1029/2000GL011956, 2001.

Jones, A. E., Wolff, E. W., Salmon, R. A., Bauguitte, S. J.-B., Roscoe, H. K., Anderson, P. S., Ames, D., Clemitshaw, K. C., Fleming, Z. L., Bloss, W. J., Heard, D. E., Lee, J. D., Read, K. A., Hamer, P., Shallcross, D. E., Jackson, A. V., Walker, S. L., Lewis, A. C., Mills, G. P., Plane, J. M. C., Saiz-Lopez, A., Sturges, W. T., and Worton, D. R.: Chemistry of the Antarctic Boundary Layer and the Interface with Snow: an overview of the CHABLIS campaign, Atmospheric Chemistry and Physics, 8, 3789–3803, doi:10.5194/acp-8-3789-2008, http://www.atmos-chem-phys.net/8/3789/2008/, 2008.

Jones, A. E., Wolff, E. W., Ames, D., Bauguitte, S. J.-B., Clemitshaw, K. C., Fleming, Z., Mills, G. P., Saiz-Lopez, A., Salmon, R. A., Sturges, W. T., and Worton, D. R.: The multi-seasonal NO_y budget in coastal Antarctica and its link with surface snow and ice core nitrate: results from the CHABLIS campaign, Atmospheric Chemistry and Physics, 11, 9271–9285, doi:10.5194/acp-11-9271-2011, http://www.atmos-chem-phys.net/11/9271/2011/, 2011.

Kuo, M. H., Moussa, S. G., and McNeill, V. F.: Modeling interfacial liquid layers on environmental ices, Atmospheric Chemistry and Physics, 11, 9971–9982, doi:10.5194/acp-11-9971-2011, http://www.atmos-chem-phys.net/11/9971/2011/, 2011.

Legrand, M., Yang, X., Preunkert, S., and Theys, N.: Year-round records of sea salt, gaseous, and particulate inorganic bromine in the atmospheric boundary layer at coastal (Dumont d'Urville) and central (Concordia) East Antarctic sites, Journal of Geophysical Research: Atmospheres, 121, 997–1023, doi:10.1002/2015JD024066, http://dx.doi.org/10.1002/2015JD024066, 2015JD024066, 2016.

McConnell, J. R., Bales, R. C., Stewart, R. W., Thompson, A. M., Albert, M. R., and Ramos, R.: Physically based modeling of atmosphere-to-snow-to-firn transfer of H2O2 at South Pole, Journal of Geophysical Research: Atmospheres, 103, 10 561–10 570, doi:10.1029/98JD00460, http://dx.doi.org/10.1029/98JD00460, 1998.

McNeill, V. F., Grannas, A. M., Abbatt, J. P. D., Ammann, M., Ariya, P., Bartels-Rausch, T., Domine, F., Donaldson, D. J., Guzman, M. I., Heger, D., Kahan, T. F., Klán, P., Masclin, S., Toubin, C., and Voisin, D.: Organics in environmental ices: sources, chemistry, and impacts, Atmospheric Chemistry and Physics, 12, 9653–9678, doi:10.5194/acp-12-9653-2012, http://www.atmos-chem-phys.net/12/9653/2012/, 2012.

Morin, S., Savarino, J., Frey, M. M., Yan, N., Bekki, S., Bottenheim, J. W., and Martins, J. M. F.: Tracing the Origin and Fate of NOx in the Arctic Atmosphere Using Stable Isotopes in Nitrate, Science, 322, 730–732, doi:10.1126/science.1161910, http://science.sciencemag.org/content/322/5902/730, 2008.

Murray, K. A., Kramer, L. J., Doskey, P. V., Ganzeveld, L., Seok, B., Dam, B. V., and Helmig, D.: Dynamics of ozone and nitrogen oxides at Summit, Greenland. II. Simulating snowpack chemistry during a spring high ozone event with a 1-D process-scale model, Atmospheric Environment, 117, 110 – 123, doi:http://dx.doi.org/10.1016/j.atmosenv.2015.07.004, http://www.sciencedirect.com/science/article/pii/S135223101530203X, 2015.

Picard, G., Libois, Q., Arnaud, L., Vérin, G., and Dumont, M.: Time-series of snow spectral albedo and superficial snow specific surface area at Dome C in Antarctica, 2012-2015, doi:10.1594/PANGAEA.860945, https://doi.pangaea.de/10.1594/PANGAEA.860945, supplement to: Picard, G et al. (2016): Development and calibration of an automatic spectral albedometer to estimate near-surface snow SSA time series. The Cryosphere, 10(3), 1297-1316, doi:10.5194/tc-10-1297-2016, 2016.

Pinzer, B. R., Schneebeli, M., and Kaempfer, T. U.: Vapor flux and recrystallization during dry snow metamorphism under a steady temperature gradient as observed by time-lapse micro-tomography, The Cryosphere, 6, 1141–1155, doi:10.5194/tc-6-1141-2012, http://www.the-cryosphere.net/6/1141/2012/, 2012.

Press, .W. H, Teukolsky, S. A., Vetterling, W. T., F.lannery, B. P.: Numerical Recipe in Fortran 90, Cambridge Univeristy Press, 2 edn., 1996.

Pruppacher, H. R. and Klett, James D., .: Microphysics of clouds and precipitation, Dordrecht ; Boston : Kluwer Academic Publishers, 2nd rev. and enl. ed edn., "With an introduction to cloud chemistry and cloud electricity.", 1997.

Röthlisberger, R., Hutterli, M. A., Sommer, S., Wolff, E. W., and Mulvaney, R.: Factors controlling nitrate in ice cores: Evidence from the Dome C deep ice core, Journal of Geophysical Research: Atmospheres, 105, 20 565–20 572, doi:10.1029/2000JD900264, http://dx.doi.org/10.1029/2000JD900264, 2000.

Sander, R.: Modeling Atmospheric Chemistry: Interactions between Gas-Phase Species and Liquid Cloud/Aerosol Particles, Surveys in Geophysics, 20, 1–31, doi:10.1023/A:1006501706704, http://dx.doi.org/10.1023/A:1006501706704, 1999.

Sander, R.: Compilation of Henry's law constants (version 4.0) for water as solvent, Atmospheric Chemistry and Physics, 15, 4399–4981, doi:10.5194/acp-15-4399-2015, http://www.atmos-chem-phys.net/15/4399/2015/, 2015.

Sazaki, G, and Zepeda S, Nakatsubo S, Yokomine. M. Furukawa. Y.: Quasi-liquid layers on ice crystal surfaces are made up of two different phases, Proc Natl Acad Sci U S A., 4, 1052–1055, doi:10.1073/pnas.1116685109, 2012.

Thibert, E., , and Dominé, F.: Thermodynamics and Kinetics of the Solid Solution of HNO3 in Ice, The Journal of Physical Chemistry B, 102, 4432–4439, doi:10.1021/jp980569a, http://dx.doi.org/10.1021/jp980569a, 1998.

Atmos. Chem. Phys. Discuss., doi:10.5194/acp-2016-1069, 2016
Manuscript under review for journal Atmos. Chem. Phys.
Published: 15 December 2016

Thomas, J. L., Stutz, J., Lefer, B., Huey, L. G., Toyota, K., Dibb, J. E., and von Glasow, R.: Modeling chemistry in and above snow at Summit, Greenland ,§? Part 1: Model description and results, Atmospheric Chemistry and Physics, 11, 4899–4914, doi:10.5194/acp-11-4899-2011, http://www.atmos-chem-phys.net/11/4899/2011/, 2011.

Toyota, K., McConnell, J. C., Staebler, R. M., and Dastoor, A. P.: Air-snowpack exchange of bromine, ozone and mercury in the springtime Arctic simulated by the 1-D model PHANTAS - Part 1 In-snow bromine activation and its impact on ozone, Atmospheric Chemistry and Physics, 14, 4101–4133, doi:10.5194/acp-14-4101-2014, http://www.atmos-chem-phys.net/14/4101/2014/, 2014.

Traversi, R., Udisti, R., Frosini, D., Becagli, S., Ciardini, V., Funke, B., Lanconelli, C., Petkov, B., Scarchilli, C., Severi, M., and Vitale, V.: Insights on nitrate sources at Dome C (East Antarctic Plateau) from multi-year aerosol and snow records, Tellus B, 66, http://www.tellusb.net/index.php/tellusb/article/view/22550, 2014.

Udisti, R., Becagli, S., Benassai, S., Castellano, E., Fattori, I., Innocenti, M., Migliori, A., and Traversi, R.: Atmospheresnow interaction by a comparison between aerosol and uppermost snow-layers composition at Dome C, East Antarctica, Annals of Glaciology, 39, 53–61, doi:doi:10.3189/172756404781814474, http://www.ingentaconnect.com/content/igsoc/agl/2004/00000039/00000001/art00010, 2004.

Ullerstam, M. and Abbatt, J. P. D.: Burial of gas-phase HNO3 by growing ice surfaces under tropospheric conditions, Phys. Chem. Chem. Phys., 7, 3596–3600, doi:10.1039/B507797D, http://dx.doi.org/10.1039/B507797D, 2005a.

Ullerstam, M., Thornberry, T., and Abbatt, J. P. D.: Uptake of gas-phase nitric acid to ice at low partial pressures: evidence for unsaturated surface coverage, Faraday Discuss., 130, 211–226, doi:10.1039/B417418F, http://dx.doi.org/10.1039/B417418F, 2005b.

Wolff, E. W., Jones, A. E., Bauguitte, S. J.-B., and Salmon, R. A.: The interpretation of spikes and trends in concentration of nitrate in polar ice cores, based on evidence from snow and atmospheric measurements, Atmospheric Chemistry and Physics, 8, 5627–5634, doi:10.5194/acp-8-5627-2008, http://www.atmos-chem-phys.net/8/5627/2008/, 2008.

Yuan-Hui, L. and Gregory, S.: Diffusion of ions in sea water and in deep-sea sediments, Geochimica et Cosmochimica Acta, 38, 703 – 714, doi:http://dx.doi.org/10.1016/0016-7037(74)90145-8, http://www.sciencedirect.com/science/article/pii/0016703774901458, 1974.